COMBINATION OF MITOCHONDRIAL AND PLASMA MEMBRANE CITRATE TRANSPORTER PROTEIN INHIBITORS TARGETS ON *DE NOVO* LIPOGENESIS SELECTIVELY INDUCING APOPTOSIS IN HEPG2 CELLS

WAN-ANGKAN POOLSRI

A Thesis Submitted to the Graduate School of Naresuan University
In Partial Fulfillment of the Requirements
for the Master of Science Degree in Physiology
May 2017

Thesis entitled "Combination of mitochondrial and plasma membrane citrate transporter protein inhibitors targets on de novo lipogenesis selectively inducing apoptosis in HepG2 cells"

by Wan-angkan Poolsri

has been approved by The Graduate School as partial fulfillment of the requirements for the Master of Science Degree in Physiology of Naresuan University

Oral Defense Committee

Jiraporn Tocharus ..... Chair

(Assistant Professor Jiraporn Tocharus, Ph.D.)

Piyarat Srisawang ..... Advisor

(Assistant Professor Piyarat Srisawang, Ph.D.)

Damrongsak Pekthong ..... Co – Advisor

(Damrongsak Pekthong, Ph.D.)

..... Internal Examiner

(Associate Professor Sutatip Pongcharoen, MD. Ph.D.)

Approved

.....

(Associate Professor Sakchai Wittaya-areekul, Ph.D.)

Associate Dean for Research and International Affairs

for Dean of the Graduate School

- 9 MAY 2017

ACKNOWLEDGEMENT

Frist of all, I would like to express my sincere thanks to my major advisor, Assistant Professor Dr.Piyarat Srisawang, for her best advice, support, caring, and providing me to be honest and patient doing the research.

I am grateful to my co-advisor and special teacher, Dr.Dumrongsak Pekthong and Associate Professor Dr.Sutatip Pongcharoen for helpful suggestions, and technical advice for my laboratory experiments.

Furthermore, I would like to thank the Faculty of Medical Science, Naresuan University for supporting grants.

I would also like to thank my friends for their friendship and always encouragement me with their best wish. Finally, I am very grateful to my family for their love and cheering me up through the good and bad time.

Wan-angkan Poolsri

Title	COMBINATION OF MITOCHONDRIAL AND PLASMA MEMBRANE CITRATE TRANSPORTER PROTEIN INHIBITORS TARGETS ON DE NOVO LIPOGENESIS SELECTIVELY INDUCING APOPTOSIS IN HEPG2 CELLS
Author	Wan-angkan Poolsri
Advisor	Assistant Professor Dr.Piyarat Srisawang, Ph.D.
Co-Advisor	Dr.Dumrongsak Pekthong, Ph.D.
Academic Paper	Thesis M.S. in Physiology, Naresuan University, 2016
Keywords	Citrate transporter, De novo lipogenesis, Apoptosis, HepG2 cells

ABSTRACT

Cancers cells switch the ATP generation pathway from oxidative phosphorylation (OXPHOS) to rely on aerobic glycolysis or Warburg effect to provide substrate precursors for the de novo lipogenesis (DNL). High rates of ATP generation and fatty acid synthesis from DNL ensure a high demand of energy and biomolecule synthesis in tumor progression. The intracellular citrate is the starting material of the DNL pathway in cancer cells. Two sources of intracellular citrate are identified which are mitochondrial and extracellular citrate. Citrate derived from mitochondrial matrix of OXPHOS pathway is transported by the mitochondrial citrate transport protein (CTP) on the inner membrane of mitochondria. Citrate is also imported from the extracellular to the cytosol via plasma membrane citrate transporter (PMCT). Inhibition of DNL pathway has been found as one of the most efficient cancer therapies by suppressing cell viability and promoting cell apoptosis in cancers. Thus, this study investigated the anti-tumor effect of CTP inhibitor and PMCT inhibitor to decrease DNL pathway leading to a reduction of cancer cell proliferation. It was found that 24 h treatment HepG2 with the CTP and PMCT inhibitor combination resulted in decrease cell viability measured by MTT assay, enhanced apoptotic cell death associated with a disruption of mitochondrial membrane potential detected by flow cytometer and caused the cell cycle arrest in S and G2/M phases with reduction of cells in G0/G1 phase. Moreover, Combination of CTP

and PMCT inhibitor inducing apoptosis was associated with down regulation carnitine palmitoyl transferase-1 (CPT-1) activity, and increase intracellular generation of reactive oxygen species (ROS). Apoptosis was also caused by suppressing of Bcl-2 activity. Thus, we speculated that apoptosis mechanism of CTP and PMCT inhibitor involved the deficiency of the DNL pathway as a result of depletion of citrate. Collectively, our findings demonstrate that the CTP and PMCT inhibitor will be potent novel anticancer treatments targeting the inhibition of the DNL pathway.

LIST OF CONTENT

LIST OF CONTENT (CONT.)

LIST OF TABLE

LIST OF FIGURE

LIST OF FIGURE (CONT.)

ABBREVIATIONS

ACC	=	Acetyl-CoA carboxylase
ACLY	=	ATP-citrate lyase
ACS	=	Acyl-CoA synthetase
AKT	=	Protein kinase B (PKB)
ATP	=	Adenosine triphosphate
ADP	=	Adenosine diphosphate
AMPK	=	AMP-activated protein kinase
Alpha KG	=	α-ketoglutarate
BCA	=	Bicinchoninic acid
CytC	=	Cytochrome C
CCD	=	Charge-coupled device
CTP	=	Citrate transport protein
CTPi	=	Citrate transport protein inhibitor
CPT-1	=	Carnitine palmitoyl transferase-1
DAPK2	=	Death-associated protein kinase 2
DMSO	=	Dimethyl sulfoxide
DNL	=	De novo lipogenesis
ETC	=	Electron transport chain
Ex/Em	=	Excitation/Emission
Fum	=	Fumarate
FASN	=	Fatty acid synthase
GF	=	Growth factor
HCC	=	Hepatocellular carcinoma
HIV	=	Human immunodeficiency virus
LCFAs	=	Long chain fatty acids
mM	=	Millimolar
MMP	=	Mitochondrial membrane potential
MPER	=	Mammalian Protein Extraction Reagent
mTORC1	=	Mammalian target of rapamycin complex 1
MUFA	=	Monounsaturated fatty acid

ABBREVIATIONS (CONT.)

NAD	=	Nicotinamide adenine dinucleotide
NADP	=	Nicotinamide adenine dinucleotide phosphate
NaCT	=	Sodium-coupled citrate transporter
NAFLD	=	Non-alcoholic fatty liver disease
NAC	=	N-Acetyl-L-cysteine
OAA	=	Oxaloacetate
PDH	=	Pyruvate dehydrogenase
PI3K	=	Phosphoinositide 3-kinase
PMCT	=	Plasma membrane citrate transporter
PMCTi	=	Plasma membrane citrate transporter inhibitor
ROS	=	Reactive oxygen species
RTK	=	Receptor tyrosine kinase
SCD	=	Stearoyl-CoA desaturase
SDH	=	Succinate dehydrogenase
SREBP1	=	Sterol regulatory element-binding protein
Suc	=	Succinate
TCA	=	Tricarboxylic acid cycle
TOFA	=	5-(tetradecyloxy)-2-furoic acid
TRAIL	=	Tumor necrosis factor-related apoptosis-inducing ligand

CHARPTER I

INTRODUCTION

Rationale of the study

The reprogramming of energy pathways in cancers switching major metabolism pathway from oxidative phosphorylation (OXPHOS) to rely on aerobic glycolysis also known as Warburg effect to ensure a high tumor progression rate. The Hallmark features of this phenomenon is that glucose uptake is increased for synthesis of biomolecules including nucleotide, amino acids, and lipids to support high proliferative phenotype of cancer (Currie E., Schulze A., Zechner R., Walther T. C., & Farese R. V., Jr., 2013). To confer rapid proliferation and survival, intermediates from OXPHOS are redirected into the de novo lipogenesis (DNL) pathway for long chain fatty acids (LCFAs) synthesis. DNL plays important roles in serving as precursors for macromolecule synthesis for highly proliferative cancer cells, more than in most normal cells for which their lipids come from the abundant levels in the circulation. The enzymes participating in DNL pathway are up-regulated or constitutively expressed in most types of cancer cells (Zaidi N., et al., 2013). DNL pathway uses cytosolic citrate exported from mitochondria and extracellular into the cytoplasm, which is then converted to acetyl-CoA by ATP-citrate lyase (ACLY) followed by carboxylation to form malonyl-CoA by acetyl-CoA carboxylase (ACC). Fatty acid synthase (FASN) uses acetyl-CoA, malonyl-CoA, and NADPH to elaborate LCFAs, especially 16-C palmitate, which is then metabolized by β-oxidation and desaturated to monounsaturated fatty acids (MUFAs), leading to the promotion of cell proliferation. Anticancer therapy targeting the DNL enzymes has been extensively studied as one of the most efficient cancer therapies that promotes cancer cell apoptosis without affecting non-transformed cells (Impheng H., Pongcharoen S., Richert L., Pekthong D., & Srisawang P., 2014). Two sources of intracellular citrate are transported by protein transporters including the mitochondrial citrate transport protein (CTP) via citrate/malate exchange that located on inner membrane of mitochondrial to efflux citrate into cytoplasm and citrate is also imported by the plasma membrane citrate transporter (PMCT) a Na+/citrate co-transporter or NaCT to influx extracellular citrate

from blood circulation across the plasma membrane into cytoplasm (Sun J., et al., 2010). Thus, inhibition of these transporters by CTP and PMCT inhibitors to decrease intracellular citrate level causes inhibition of the DNL pathway and reduction of cell proliferation, leading to the induction of apoptosis in hepatocellular carcinoma HepG2 cell.

Main objectives

The present study was aimed to evaluate the effect of the combination of the CTP and PMCT inhibitors on inhibition of de novo lipogenesis pathway that led to the induction of apoptosis in HepG2 cells.

Specific objectives

1. To evaluate the effect of CTP or PMCT inhibitor alone and their combinations on HepG2 cell growth and proliferation.
2. To determine the effect of CTP and PMCT inhibitors and their combinations on de novo lipogenesis pathway in HepG2 cell
3. To determine the effect of CTP and PMCT inhibitors and their combinations on apoptosis pathway in HepG2 cell

The scope of the study

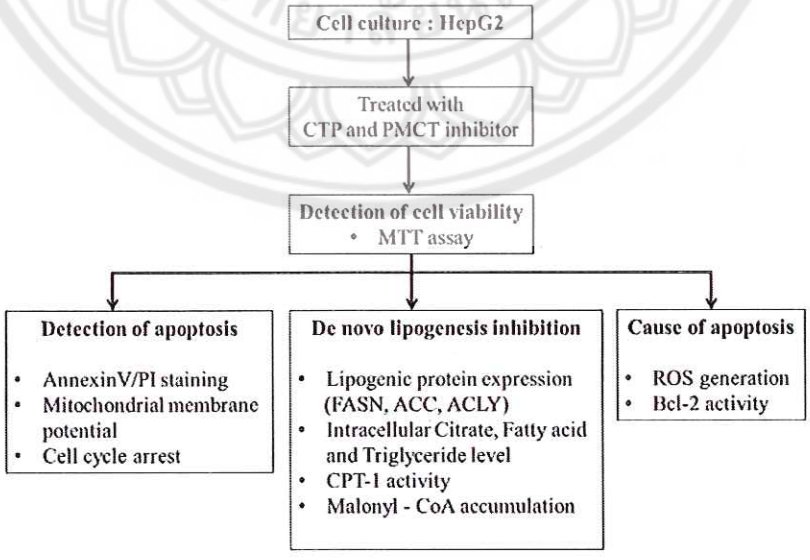

Figure 1 Conceptual research framework

Hypothesis

The combination of CTP and PMCT inhibitors could reduce intracellular citrate, fatty acid, and triglyceride, thus the decreasing of substrate and product of de novo lipogenesis pathway lead to apoptosis of HepG2 cells. The mechanism of apoptosis effect of combined inhibitor would be possible involved either the deficiency of product fatty acid level or the enhancement of ROS production.

Keywords

Citrate transporter, De novo lipogenesis, Apoptosis, HepG2 cells

Expected outcomes of the research

The present study will demonstrate that inhibition of citrate transporters by the combination of CTP and PMCT inhibitors suppresses DNL fatty acid synthesis resulting in mitochondrial dysfunction and inducing HepG2 apoptosis cell death. Additionally, a result of inhibiting CPT-1 activity will be a mechanism characterized as up-regulated expression of pro-apoptotic factors. The present study will show that suppression of citrate transporter-induced apoptosis will restrict to cancer cells while normal hepatocyte cells will be resistance. Thus, this study will propose that the CTP and PMCT inhibitors may be a novel and selective anticancer therapy that targets the inhibition of the de novo lipogenesis. In addition, mitochondrial dependent apoptotic induction will be found concomitantly with increase ROS generation, which implies that mitochondria are defined as a source of ROS-triggered apoptosis in HepG2 cells. The present study will also suggest that high ROS level significantly reaches severe oxidative damage to many cellular biomolecule functions that work in concerted action to participate in growth arrest and cell death, leading to apoptotic induction following DNL suppression in HepG2 cells. This research will further suggest that the ability to selectively inhibit DNL pathway may be a novel therapeutic of metabolic disorders resulting from the synthesis of excess lipid, cholesterol, and glucose, including human obesity, hyperlipidemia, hyper-cholesterolemia, and type 2 diabetes.

CHARPTER II

LITERATURE REVIEWS

Cancer

Definition of cancer is the cells having an abnormal growth caused by multiple changes in gene expression leading to dysregulating balance of cell proliferation and cell death (Ruddon R. W., 2007). Without adequate control of cellular proliferation processes, cancer can invade tissues and metastasize to distant sites, causing significant morbidity. Most type of cancers are classified into 4 stages, stage I to stage IV. The identity of each stage is important to cancer has a predictable, ineluctable progression. Although some tumors may progress in a stepwise from a small to a larger primary tumor, and then spread to local nodes and distant sites, others may spread to local nodes or have microscopic and clinically undetectable. Although the exact criteria used vary with each organ site, the staging categories listed below represent a useful generalization (Ruddon R. W., 2007).

Stage I: The primary tumor is limited to the organ of origin. There is no evidence of esophageal or colorectal transmission. The tumor can be removed by surgery. Long-term survival rate is 70% to 90%.

Stage II: The primary tumor has capability to spread to surrounding tissues and lymph nodes immediately. However, due to the local spread, it may not be fully measurable. Survival rate is 45% to 55%.

Stage III: The large primary tumor that have grown more deeply into nearby tissue associated with a diameter of 3 cm. They may have also spread to lymph nodes but not to other parts of the body. Survival rate is 15 to 25%.

Stage IV: Extensive primary tumor (may be more than 10 cm in diameter) invades the surrounding tissue or wide spreads to other organs or parts of the body, and there is evidence of distant metastasis beyond the primary tumor tissue. Survival rate is below 5%.

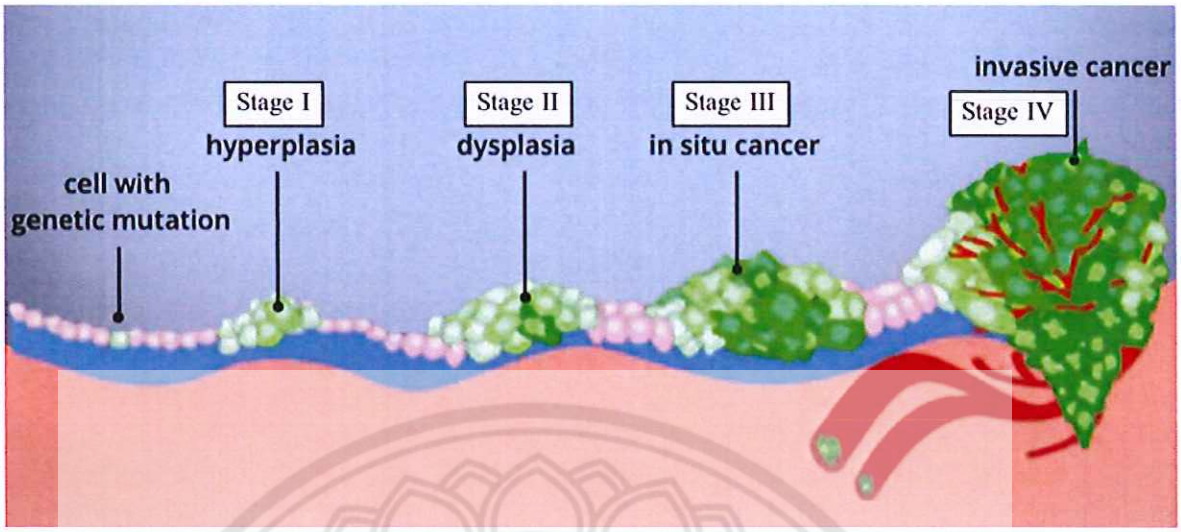

Figure 2 the four stages of cancer

Source: https://thetruthaboutcancer.com/understanding-four-stages-cancer

Treatment of cancer including surgery, radiotherapy, and chemotherapy are the major principles of current cancer therapies. Treatment options depend on the type of cancer, stage, and health status of patients. The aim of treatment is to kill as many cancerous cells while reducing damage or side effects to normal cells nearby. Advances in technology make this possible. The three main treatments are

1. Surgery: directly removing the tumor
2. Chemotherapy: using chemicals to kill cancer cells
3. Radiation therapy: using X-rays to kill cancer cells

The future of cancer treatment lies in providing patients with an even greater level of personalization. The beginning to treatment is the offer treatment options based on the genetic changes occurring in a specific tumor (Ruddon R. W., 2010).

Metabolic differences between normal and cancer cells

The earliest studies focused on cancer biology, molecular changes in the signaling pathways that caused uncontrolled proliferation. However, in recent years, more evidence has shown that reprograming metabolism can be an important process during tumorigenesis. The variability of the metabolism required for the normal cells

shift to cancer cells for supporting malignant growth (Lu J., Tan M., & Cai Q., 2015). In normal cells, glucose is catabolized to pyruvate. Pyruvate is further converted to acetylo-CoA and oxidized to carbon dioxide through the mitochondrial tricarboxylic acid (TCA) cycle, which generates NADH and FADH2. The transfer of electrons from NADH and FADH2 to oxygen through respiratory chain is an energy-efficient process. Together, glycolysis, TCA cycle, and electrons transfer phosphorylation produce 36 ATP molecules per glucose molecule. In cancer cells, oxidative phosphorylation is inhibited and cells use glycolysis to provide them with the necessary energy. Glycolysis can only provide 2 ATP molecules per glucose molecule and produce lactic acid as the end product. Cancer cells preferentially use glycolysis even in the abundance of oxygen whereas normal cells use only when oxygen supply is limited. The increased glucose uptake with concomitant lactate production, even under aerobic conditions, is known as the Warburg effect or aerobic effect (Vander Heiden M. G., Cantley L. C., & Thompson C. B., 2009).

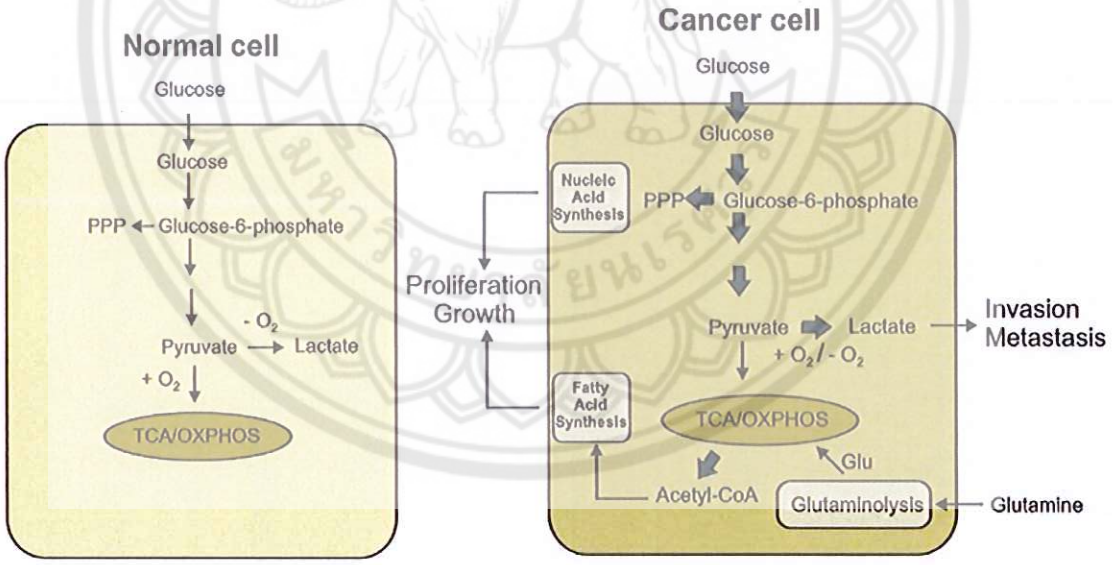

Figure 3 Metabolic differences between normal and cancer cells

Source: Jozwiak P., Forma E., Brys M., & Krzeslak A., 2014

The increase in glycolytic flux is very important to cancer cells because glycolytic intermediates affect many biological processes that produce novo nucleotides, lipids, amino acids, and NADPH. Reprograming of cellular metabolism in the cell for the synthesis of precursors for small molecules allows for the accumulation of biomass during growth and cell expansion (Lunt S. Y. & Vander Heiden M. G., 2011). In addition, cancer cells are more resistant to hypoxia-related tumor growth conditions by switching their metabolism from oxidative phosphorylation to oxygen-independent glycolysis (Semenza G. L., 2011). Cancer cells can reduce the pH of the environment around outside of the cell by increasing the lactic acid, activating the metallo protease activity and helping to degrade the matrix components outside the cell. Thus, lactate may act as a catalyst for invasion and spread of cancer (Kato Y., et al., 2005; Martinez-Outschoorn U. E., et al., 2011). The molecular mechanisms that control metabolic reprograming in cancer cells are complex. Tumors conduct aerobic glycolysis and upregulate glutaminolysis, pentose phosphate pathway (PPP), and fatty acid synthesis or de novo lipogenesis (DNL), in partially associated the activation of oncogenes or loss of tumor suppressor activity.

De novo lipogenesis in cancer

De novo lipogenesis (DNL) or de novo fatty acid synthesis is the metabolic pathway that synthesizes fatty acids from excess carbohydrates. These fatty acids can then be incorporated into triglycerides (TGs) for energy storage. In normal conditions DNL mainly takes place in liver and adipose tissue.

The flow of carbons from glucose enters the glycolytic pathway and generates pyruvate. This pyruvate is converted into acetyl-CoA that feeds the tricarboxylic acid (TCA) cycle. The citrate produced from TCA cycle exits the mitochondrion to DNL pathway, which is modulated by lipogenic enzyme the first step of the pathway is the conversion of citrate to acetyl- CoA by ATP-citrate lyase (ACLY). The resulting acetyl-CoA is carboxylated to malonyl-CoA by acetyl-CoA carboxylase (ACC). Fatty acid synthase (FASN) is the key rate-limiting enzyme that brings about the conversion of malonyl-CoA into the production of 16-carbon saturated palmitate. After a series of reactions, palmitate is further converted into complicated fatty acids. The main product of DNL is palmitate but stearate and shorter fatty acids are also generated.

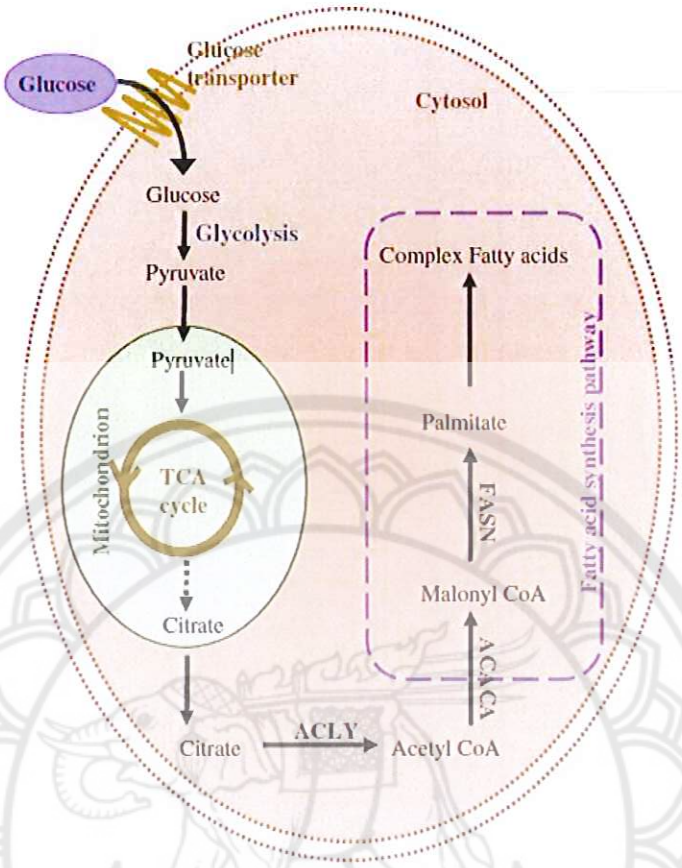

Figure 4 De novo lipogenesis pathway

Source: Ameer F., Scandiuzzi L., Hasnain S., Kalbacher H., & Zaidi N., 2014

Regulation of de novo lipogenesis has been shown to highly significantly responds to changes in dietary regimen. For example, high carbohydrate diets can cause an increase in DNL in the liver that results in an elevated hypertriglyceridemia. Carbohydrate intake is not only the quantity diet but also the type of dietetic carbohydrate that affect DNL pathway. Fructose, in particular, has been identified as a monosaccharide with an especially potent effect on DNL. It has been shown that simple sugars are more effective than complex carbohydrates in stimulating hepatic DNL. Lipogenesis in the adipose tissue is less responsive than hepatic DNL to acute or prolonged carbohydrate overfeeding (Diraison F., et al., 2003). Deregulations in the lipogenic pathway are observed in certain pathological or physiological conditions. The DNL abnormalities in lipogenic tissues that cause major can damage the usual lipid

balance of body. In addition to the non- lipogenic tissue that DNL is suppressed under normal conditions could exhibit up-regulate of this pathway. This inappropriate activity of lipogenesis in ordinarily non lipogenic tissues could be caused by viral infections or by malignant transformation of normal cells (Ameer F., et al., 2014).

De novo lipogenesis in cancer is one of the most important metabolic hallmarks of cancer cells. Depending on the tumor type, tumor cells synthesize up to 95% of saturated and mono-unsaturated fatty acids (MUFA) de novo in spite of sufficient dietary lipid supply. It is suggested that activation of DNL is required for carcinogenesis and for tumor cell survival. Fatty acids support various aspects of tumorigenesis by multiple mechanisms. The most widely discussed aspect of fatty acids (FAs) biochemistry with respect to tumor biology is their role as building blocks for newly-synthesized membrane phospholipids. Large amounts of FAs are required to accommodate high rates of proliferation in cancer cells (Strable M. S. & Ntambi J. M., 2010). Cancer cells can acquire FAs through DNL pathway to support their growth and proliferation.

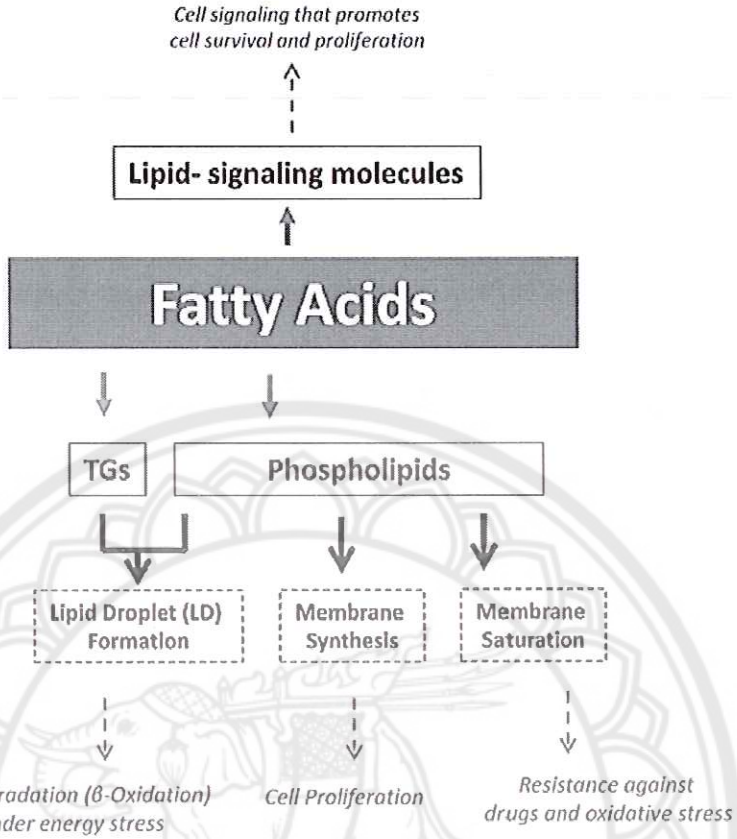

Figure 5 Fatty acids promote tumor cell development, progression and survival

Source: Zaidi N., et al., 2013

Thus, the increased DNL pathway promotes cell membrane synthesis of cancer cells with monounsaturated and unsaturated fatty acids. Because these lipids tend to produce less lipids peroxidation than the polyunsaturated acyl complex, DNL offers the ability of cancer cells to more resistant from oxidative stress which induces cell death. In addition, saturated fatty acids from lipogenesis are more densely, increased lipogenesis also changes the transverse membrane dynamics that may limit uptake of drugs, making cancer cells resistant to treatment (Rysman E., et al., 2010). Fatty acids may be used to supply energy. Most of tumors show highly rate of glucose uptake, which supports biosynthetic requirements and biological synthesis. However, certain type of tumors including prostate tumors, show an increased dependence on β-oxidation of fatty acids as their primary energy source. Prostate tumor has low uptakes of glucose,

increased fatty acid uptake, and expression of certain enzymes associated with β-oxidation (Effert P. J., et al., 1996; Liu Y., Zuckier L. S., & Ghesani N. V., 2010). Fatty acids can also be used for the biosynthesis of an array of protumorigenic lipid signaling molecules. A lipid messenger considered to be particularly important in contributing to cancer is phosphatidylinositol-3, 4, 5-trisphosphate, a molecule that is formed by the action of phosphatidylinositol-3-kinase (PI3K) and activates protein kinase B/Akt to stimulate cell proliferation and survival (Yuan T. L. & Cantley L. C., 2008). Other prominent examples of lipid messengers are lysophosphatidic acid (LPA) that signals through a family of G protein coupled receptors to promote cancer aggressiveness, and prostaglandins, a class of lipid messengers that are formed by cyclooxygenases and support migration and tumor-host interactions (Mashima T., Seimiya H., & Tsuruo T., 2009; Ren J., et al., 2006).

Hepatocellular carcinoma

Hepatocellular carcinoma (HCC) is principal becoming a common global causing of cancer deaths. HCC the fifth commonest malignancy and arises most frequently in patients with cirrhosis and it is dominant feature of primary hepatic tumor. The incidence of HCC is the highest observed in South East Asian including Thailand (GLOBOCAN, 2012). Independent risk factors of cirrhosis and HCC are Hepatitis B virus (HBV) infection and Hepatitis C virus (HCV) infection. The global distribution of HCC is disproportionate, being most common in areas where chronic HBV infection is highly prevalent. However, HCC is an increasing problem in the western world, due to migration from HBV-endemic regions, HCV infection, Other risk factors are including alcohol cirrhosis, non-alcoholic steatohepatitis, and associated to obesity epidemics (Kim J. U., et al., 2016).

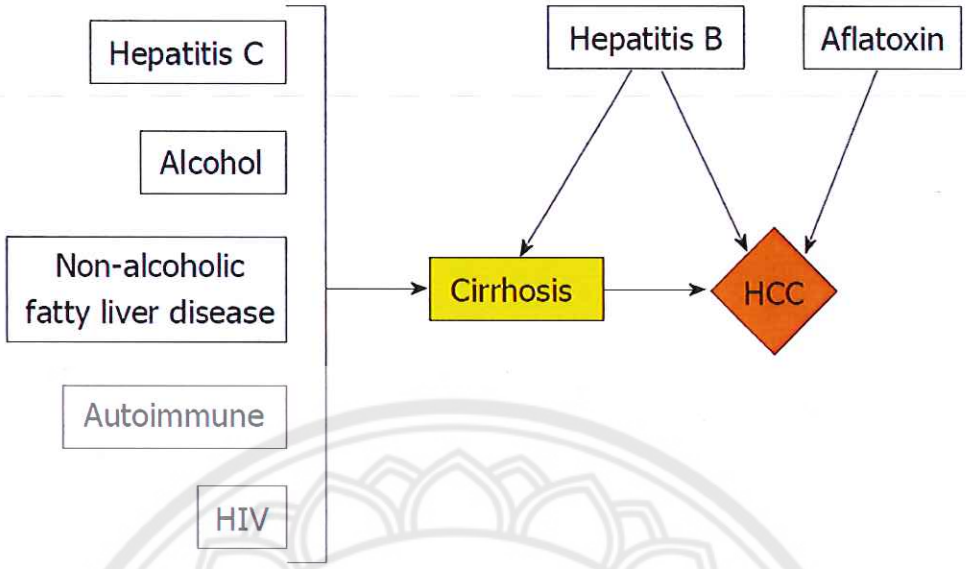

Figure 6 Independent risk factors of cirrhosis and HCC HIV: Human immunodeficiency virus; HCC: Hepatocellular carcinoma

Source: Kim J., et al., 2016

In previous research has demonstrated that pathophysiology of HCC generally arises in the background of cirrhosis and relates to metabolic syndrome with insulin resistance. The insulin resistance is principal dominator that links all of the metabolic syndromes including (Paschos P. & Paletas K., 2009). The gene expression of IRS-1, TNF-alpha, PPAR, and PI3K signaling leading to free fatty acids flux and accumulation of the fatty liver can develop HCC. Additionally, obesity and life style causing of hyperglycemia and hyperinsulinemia can induce cirrhosis and HCC via insulin resistance (Rahman R., Hammoud G. M., Almashhrawi A. A., Ahmed K. T., & Ibdah J. A., 2013). These factors that are associated with development of the metabolic syndrome and HCC maybe inherently linked. It has been established that insulin resistance exerts a major role in the development of NAFLD even in lean subjects with appropriate glycemic control (Gaggini M., et al., 2013). Insulin resistance leads to fat accumulation in the hepatocytes by lipolysis and hyperinsulinemia. The accumulation of abnormal adipose tissue, that release of pro-inflammatory cytokines, inhibition of the

anti-inflammatory cytokines and lipotoxicity together, promote the insulin resistance of the hepatocyte cause to hyperinsulinemia (Ahsan M. K., et al., 2009).

Several mechanisms have been proposed that may work equally well for tumors promoting the environment in the metabolic syndrome, which may differentiate between the HCC pathology variants associated with NAFLD from the association of infectious and alcoholic diseases. Hyperinsulinemia results in increased insulin growth factor-1 (IGF-1) which has important proliferative and anti-apoptotic effects. Up-regulation in IGF-1/IRS1 pathway has been shown to contribute to the pathogenesis of HCC. Likewise, peroxisome proliferator-activated receptors (PPARs) regulate a network of genes encoding protein involved in fatty acids uptake, enzymes required for the β-oxidation of fatty acids, and enzymes required for ketogenesis. Expansion of adipose tissue in obesity may lead to release of pro-inflammatory cytokines. Visceral fat accumulation has been shown to be an independent risk factor for HCC recurrence after curative treatment (Ohki T., et al., 2009; Tomimaru Y., et al., 2013). Further, Interleukin-6 (IL-6) has been linked to obesity associated inflammatory response potentiating cell proliferation and anti-apoptotic mechanisms. Tumor necrosis factor (TNF) activates pro-oncogenic pathways including JNK, NF-kB, mTOR, and the extracellular signal-regulated kinases promote HCC growth in mice. Both dietary and genetic obesity promote liver inflammation and tumorigenesis by enhancing IL-6 and TNF expression (Park E. J., et al., 2010).

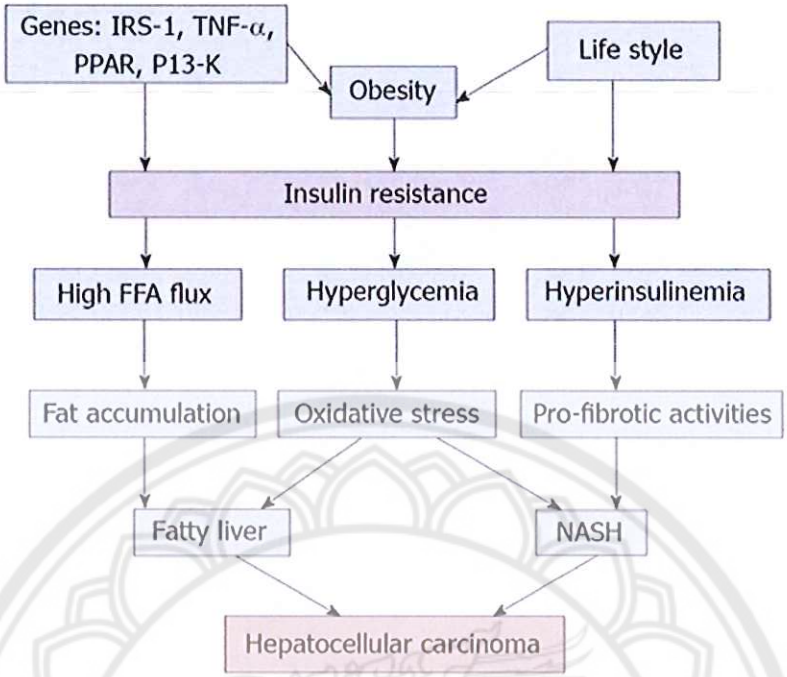

Figure 7 Hepatocellular carcinoma associated with the metabolic syndrome

Source: Rahman R., et al., 2013

Citrate transport protein

1. Citrate transport protein (CTP)

   Synonym: SLC25A1 (CiC or CTP)

   Citrate/Malate exchange; Electrogenic transport

   Activity: High activity in liver and absent in other tissues (Sluse F, 1971)

   mRNA and/or protein levels

   High: liver, pancreas, and kidney

   Low or absent: brain, heart, skeletal muscle, placenta, and lungs (Huizing M, 1998)

2. Plasma membrane citrate transporter (PMCT)

   Synonym: SLC13A5 (NaCT or PMCT)

   Sodium-citrate co-transporter; Facilitated diffusion

   Expression: high level in plasma membrane of mammalian liver, and lower levels in the brain and testes (Katsuhisa I, 2002)

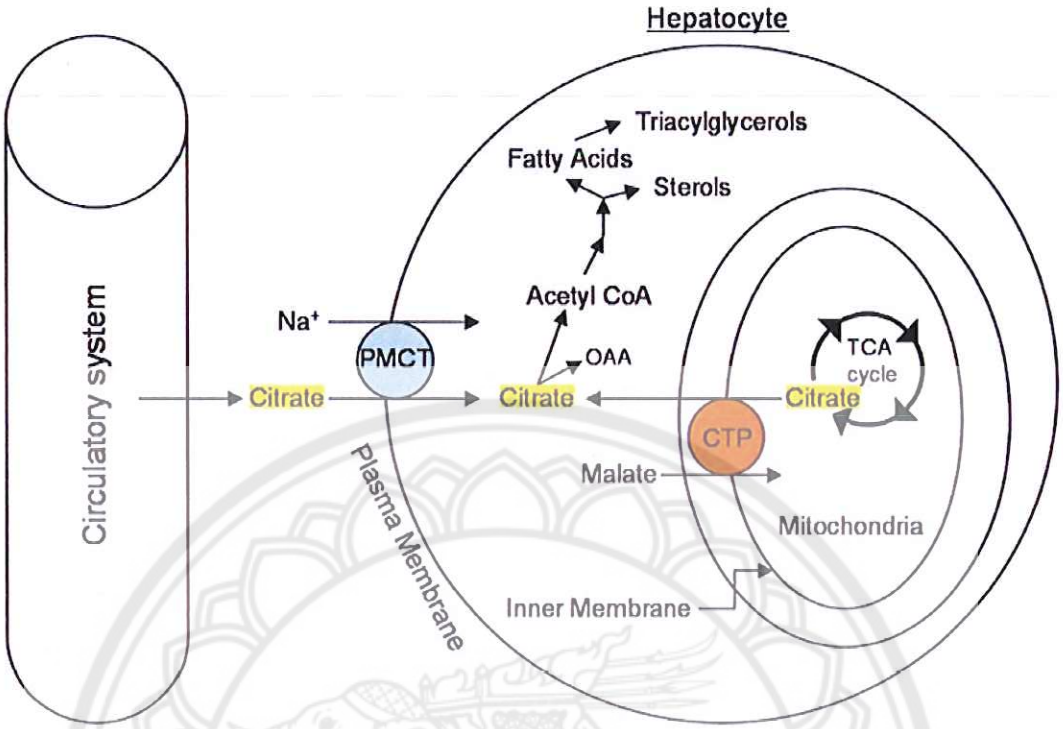

Figure 8 Schematic depiction of the roles of the PMCT and the CTP in supplying citrate to fuel hepatic fatty acid, triacylglycerol, and sterol biosynthesis

Citrate transport protein (CTP) inhibitor

Synonym: ZINC Compound 792949

4-Chloro-3-[[(3-nitrophenyl) amino]sulfonyl]-benzoic acid

Formula: $C_{13}H_9ClN_2O_6S$

Molecular Weight: 356.74

Figure 9 Structure of mitochondrial citrate transport protein (CTP) inhibitor

CTP inhibitor is an inhibitor of mitochondrial citrate transport protein. The transporter catalyzes citrate/malate exchange with citrate moving outward across the inner membrane of mitochondria (Xu Y., et al., 2000). The previous studies have reported about characteristics of the transporter which was originally studied in yeast model. In The CTP in yeast is thought to catalyze a citrate/isocitrate exchange. Recently, it has reported the discovery of compounds that inhibit CTP activity via in silico screening of the ZINC database (Sun J., et al., 2010). Furthermore, CTP as a target of p53 mutation (tumor suppressor gene), improve survival rate, and reduce chemotherapy resistance in cancer (Kolukula V. K., et al., 2014).

Plasma membrane citrate transporter (PMCT) inhibitor

Synonym: ZINC Compound 39396

2-(phenylmethylthio)-N-(2-pyridylmethyl)propanamide

Formula: C16H18N2OS

Molecular Weight: 286.4

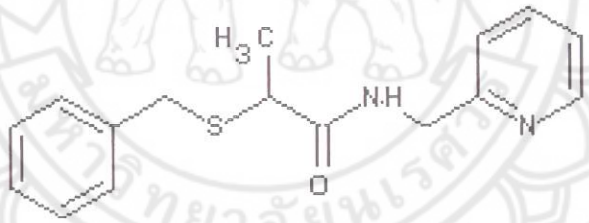

Figure 10 Structure of plasma membrane citrate transporter (PMCT) inhibitor

In 2010 Sun J. analyzed the inhibitor of PMCT, which derived from ZINC compound 39396 (69% inhibition of PMCT). The transporter is located on the plasma membrane of human and rat liver (Klingenberg M., 1972), rat and mouse brain (Robinson B. H., Williams G. R., Halperin M. L., & Leznoff C. C., 1971), Drosophila melanogaster (Kolukula V. K., et al., 2014), and Caenorhabditis elegans . This transporter catalyzes a sodium-coupled citrate transporter. It has been named NaCT and belongs to SLC13 gene family, in human NaCT referred to as SLC13A5 gene with high affinity for citrate. The transporter has been originally discovered in Drosophila known

as INDY (I'm Not Die Yet) gene. Recently, it has reported that the eukaryotic NaCT and the Drosophila INDY gene significantly alter the energy balance within variety of organisms. In addition, inhibition of NaCT to reduce citrate flux from plasma into the liver and lower intracellular citrate level lead to promoting the glycolysis pathway and reducing lipogenesis and gluconeogenesis

De novo lipogenesis pathway on apoptosis

Mechanism of apoptosis, apoptosis is the programme of cell death, which processes for non-inflammatory. The pathway of apoptosis is an integral part in biologic events such as morphology change and activation of effector call caspases, which involve in termination of cellular disassembly. The mechanism of apoptosis is complex. There are many factors have been identified to play a vital role in apoptosis. The two main pathways of apoptosis are extrinsic and intrinsic pathway. The first, extrinsic pathway begins a cytotoxic immune cell produce pro-apoptotic ligands such as Apo2L /TRAIL. The ligand binds to pro-apoptotic receptor on the surface of cell membrane. Then, it induces the adapter protein, Fas-Asscociated Death Domain (FADD) and forming a Death Inducing Signalling Complex (DISC). This process activates caspase 8, 10 and stimulates the effector caspase 3, 6. The second pathway is intrinsic pathway where cellular stress such as chemotherapeutic, ROS, UV, and hypoxia activate the p53 tumor suppressor protein to upregulate Bax/Back to turn into activated pro-apoptosis protein. Bax/Bak permeabilize the outer membrane of mitochondria to enhance efflux of cytochrome C. It will bind to adaptor Apaf-1 Then; it activates caspase 9 and effector caspase 3, 6, and 7. Bothof two main pathways of apoptosis lead to perform apoptotic cell death via phagocytosis of apoptotic bodies (Ashkenazi A., 2008).

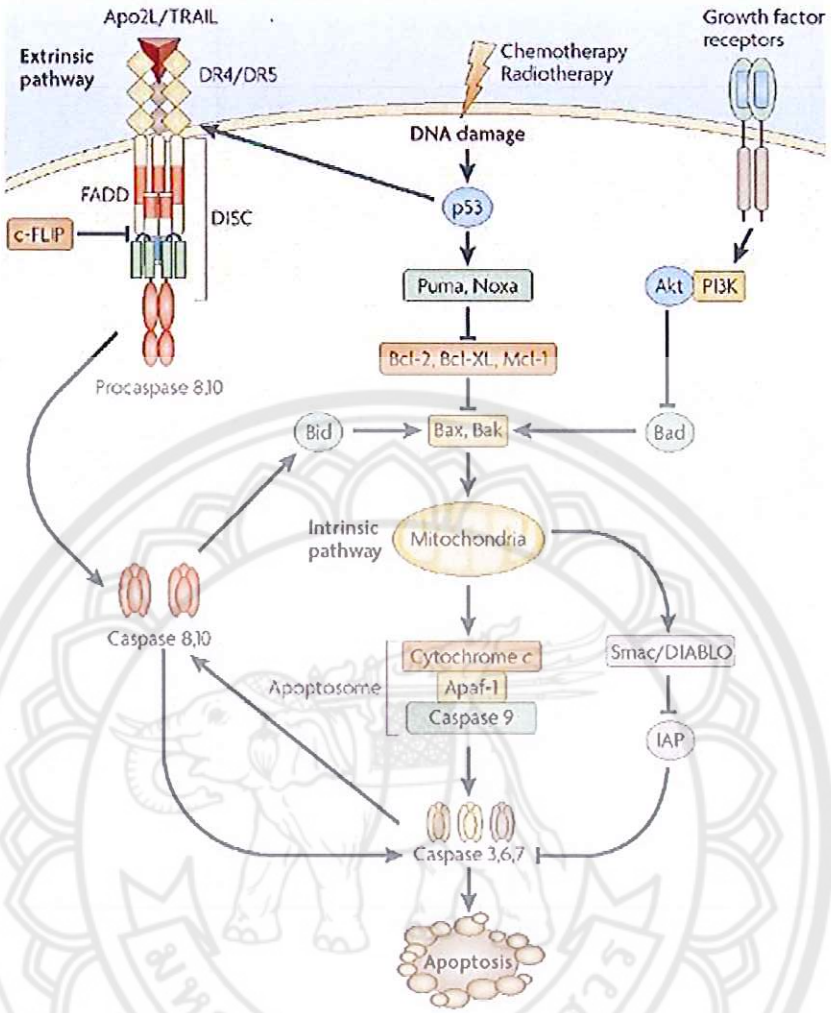

Figure 11 Apoptosis pathway

Source: Ashkenazi A., et al., 2008

Preceding attempts to exploit cancer fatty acid requirements for therapeutic benefit mainly focused on de novo lipogenesis. Several research has reported that therapeutic targeting of various enzymes of DNL pathway such as ACLY, FASN, and ACC may result in tumor regression both in vitro and in vivo. For example, the ultimate role of fatty acid synthase (FASN) a key lipogenic enzyme catalyzing the terminal steps in the de novo biogenesis of fatty acids in cancer pathogenesis. The effects that occur after fatty acid synthase (FASN) inhibit produce potent inhibition of DNA replication leading to a block in the cell cycle before G1, effective at initiating apoptosis in tumor

cells with non-functioning p53, whereas cells with intact p53 function tend to exhibit cytostatic responses and Inhibition of FASN results in the downregulation of Akt, which precedes the induction of tumor cell apoptosis in vitro and in vivo, suggesting a potential mechanism for FASN inhibition-related cell death. (Menendez J. A. & Lupu R., 2007)

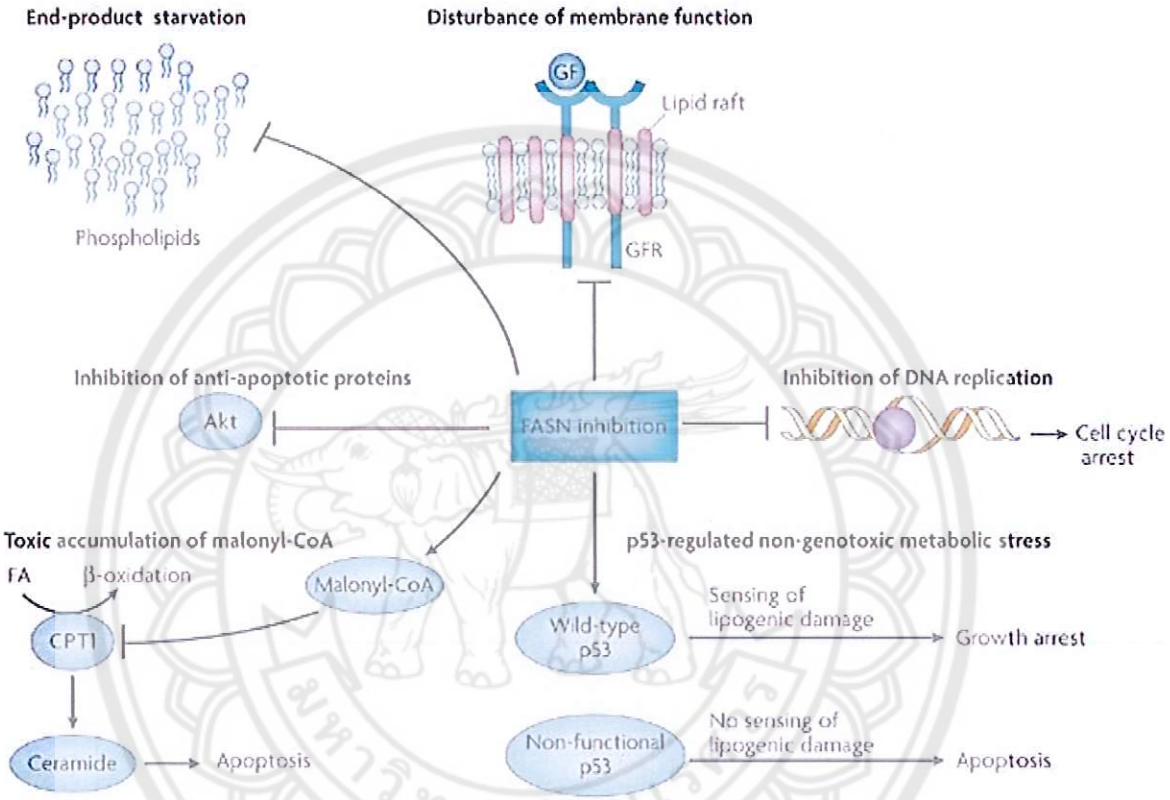

Figure 12 De novo lipogenesis (FASN inhibition) and cancer cell death

Source: Javier A., et al., 2007

Reactive Oxygen Species Generation

Oxygen Reactive Oxygen (ROS) is the result of both internal and external stimuli. Recent evidence suggests that these ROS play an important role in more physiological and pathological processes. Although high levels of ROS can cause cancer and other diseases related to oxidative damage, proposed ROS levels will be essential for cell survival, apoptosis and differentiation (Droge W., 2002). Consistently, signaling

proteins such as NF-κB, PI3-K, MAPK, and p53 play a role in cellular responses to ROS generation (Martindale J. L. & Holbrook N. J., 2002). Additional, it has been also studies in many different type of cell about the relationship between hydrogen peroxide (H2O2) and cell growth of mammalian cell. For example, reducing internal ROS levels by increasing or over-expression of antioxidant proteins to inhibiting smooth muscle cell and tumor cells proliferation (Caporossi D., Ciafre S. A., Pittaluga M., Savini I., & Farace M. G., 2003; Stone J. R. & Collins T., 2002). Significantly, the inhibition of internal ROS induced G1 cell arrest, indicating that the level of ROS steady-state level required for entry into the S phase (Sekharam M., Trotti A., Cunnick J. M., & Wu J., 1998). The production of ROS required for redox signaling is mainly attributable to NADPH oxidase and various growth factors, and cytokines stimulate ROS production by stimulating of this enzyme. Although the mitochondrial ROS generation causes redox signals are not much well known. But it has more evidence clear that H2O2 was released for the cytosol to participate in signal networks such as cell cycle change and redox balance (Kowaltowski A. J., de Souza-Pinto N. C., Castilho R. F., & Vercesi A. E., 2009). The objective of this review is to discuss the regulation of ROS production from mitochondria, cytochrome p450, and NADPH oxidase and the implications in cellular signaling.

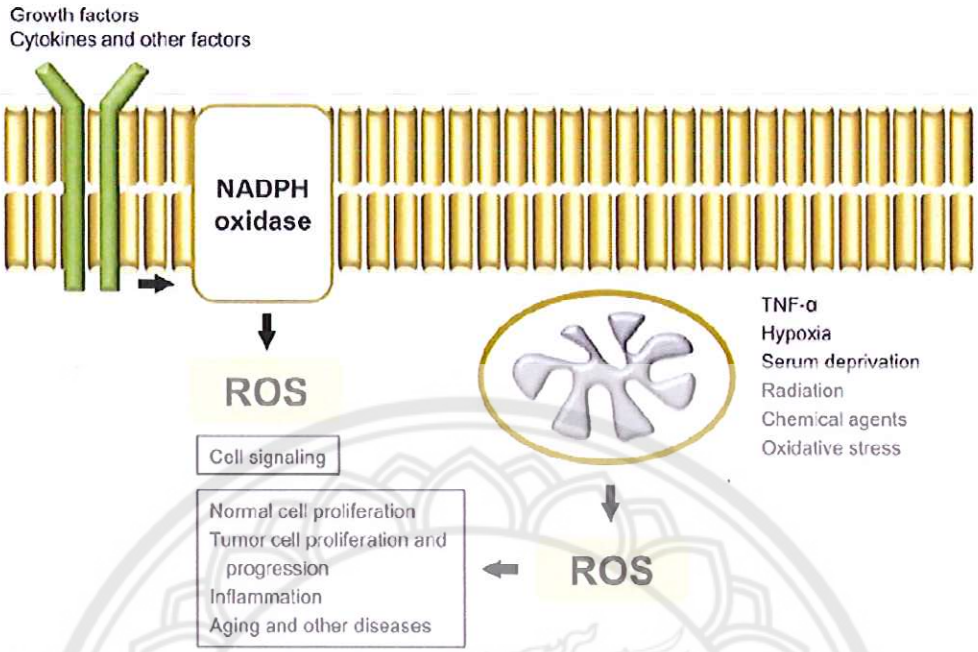

Figure 13 ROS accumulation in response to various stimuli

The mitochondria sense to external signals and pressures to stimulate release mitochondrial ROS to cytosol. Mitochondrial ROS required for normal cell function However, deviation of mitochondrial ROS regulation or releasing to cytosol is involved in many diseases, especially those associated with inflammation.

CHAPTER III

RESEARCH METHODOLOGY

Chemical and reagent

EMEM (Eagle's Minimum Essential Medium) (Corning, Manassas, VA, USA)

FBS (Fetal bovine serum), 100 IU/ml Penicillin and 100 μg/ml Streptomycin (Gibco, MA, USA)

CTP inhibitor (4-chloro-3-[(3-nitrophenyl) amino] sulfonyl benzoic acid) (ChemBridge Corporation #6652048)

PMCT inhibitor (2-(benzylsulfanyl)-N-[(pyridin-2-yl) methyl] propanamide) (TimTec ID ST056138)

MTT (3-(4, 5-dimethylthiazol-2-yl)-2,5-diphenyltetrazolium bromide) and Dimethyl sulfoxide (DMSO) (AMRESCO, Solon, OOH, USA)

Cell Cycle assay kit, Annexin V and dead cell assay kit and Bcl-2 activation dual detection kit (Merck Millipore, Germany).

JC-1 dye (5, 5′, 6, 6′-tetrachloro-1, 1′, 3, 3′-tetraethyl benzimi- dazolyl carbocyanine iodide) (Life Technologies, Thermo Scientific, NY, USA),

MPER (Mammalian Protein Extraction Reagent) (Thermo Fisher Scientific Inc., Rock ford, IL, USA)

BCA protein assay kits (Thermo Scientific, Rock ford, IL, USA).

Anti-FASN (Abcam, Biomes Diagnostic CO., Ltd, Thailand), anti-ACC (Merck Millipore, Germany), anti-ACLY and anti-β actin (Cell Signaling Technology Inc., USA)

Citrate bioAssay kit, Free fatty acid bioAssay kit and Triglyceride quantification bioassay kit (US Biological; Life Sciences, Salem, MA, USA).

CM-H_2DCFDA (5-(and-6)-chloromethyl-2', 7'-dichlorodihydrofluorescein diacetate, acetyl ester) (Thermo Fisher Scientific Inc, MA, USA)

TOFA (5-(tetradecyloxy)-2-furoic acid) (Abcam, Biomes Diagnostic,Thailand)

NAC (N-Acetyl-L-cysteine) (Sigma-Aldrich, Germany)

Instrument

Laminar flow class II biohazard (Sanyo MCV-B131F)

CO_2 incubator (Sanyo mco-20aic)

Inverted microscope (Olypus, 1x71)

High Speed Refrigerated Centrifuge (ScanSpeed, Model 2236R)

Microplate reader (Synergy HT Multi-Mode, BioTek® Instruments, Inc)

Muse cell analyzer (Merck Millipore, Germany).

Sonicator (Sonice, VCX130)

FACSCalibur flow cytometry (Becton Dickinson (BD))

CCD camera (Bio-Rad, ChemiDoc XRS+)

Mini-PROTEAN® Tetra Vertical Electrophoresis Cell and Semi-Dry Transfer Cell (Bio-Rad Laboratories, Inc.)

Methods

1. **HepG2 cell culture**

HepG2, human hepatocellular carcinoma cells, were purchased from the American Type Culture Collection (HB-8065; ATCC, Manassas, VA, USA). Cells were cultured in Eagle's Minimum Essential Medium (EMEM) (Corning, Manassas, VA, USA) with 10% fetal bovine serum (FBS) (Gibco, MA, USA) and 1% of 100 IU/ml penicillin and 100 µg/ml streptomycin (Gibco, MA, USA). The culture was routinely maintained in a 5% CO2 with 95% humidifier incubator at 37°C. Subculture was performed when culture was reached 70-90% confluence.

2. **MTT assay for detection of cell proliferation**

HepG2 cells were seeded in 96-well culture plates at a density of 3×104 cells/150 µl/well for 24 h. Then, cells were incubated with varies concentrations of 4-chloro-3-[(3-nitrophenyl) amino] sulfonyl benzoic acid (CTP inhibitor) (ChemBridge Corporation #6652048), 2-(benzylsulfanyl)-N-[(pyridin-2-yl) methyl] propanamide (PMCT inhibitor) (TimTec ID ST056138) and their combinations. After 24 h treatment, 3-(4,5-dimethylthiazol-2-yl)-2,5-diphenyltetrazolium bromide (MTT) solution of 5 mg/ml final concentration in phosphate-buffered saline (PBS) was added to each well and incubated for 3 h. The formazan crystals were dissolved in DMSO and cell viability

was then quantified by measuring absorbance at 595 nm using microplate reader (Synergy HT Multi-Mode, BioTek® Instruments, Inc).

3. Flow cytometry analysis for detection of apoptosis

Apoptotic cell was determined using Muse annexin V and dead cell assay kit (Merck Millipore, Germany). The assay is based on the detection of phosphatidylserine (PS) on the surface of apoptotic cells, using fluorescent labeled annexin V in combination with the dead cell marker, 7-AAD. Briefly, HepG2 cells were seeded in 24-well plates at a density of 3×105 cells/750 µl/well and incubated for 24 h. Subsequently, cells were exposed to CTP inhibitor and PMCT inhibitor alone and their combinations at the indicated IC50 concentrations. After treatment, cells were harvested, re-suspended in PBS, added the reagent from assay kit, mixed and incubate in the dark for 20 min at room temperature. Apoptotic stained cells were detected by Muse cell analyzer (Merck Millipore, Germany).

4. Determination of mitochondrial membrane potential (ΔΨm)

The loss of ΔΨm in HepG2 cells and primary cells were assessed by flow cytometry using JC-1 dye (5,5′,6,6′-tetrachloro-1,1′, 3, 3′-tetraethylbenzimidazolylcarbocyanine iodide) (Thermo Scientific, NY, USA), a mitochondrial membrane potential probe which enters selectively in mitochondria. The JC-1 aggregated forms accumulate inside mitochondria in response to changing of ΔΨm. Some healthy mitochondria in polarized state exhibits red fluorescence emission with high aggregates JC-1 forms in the mitochondrial matrix while it remains monomeric form in the cytoplasm with depolarized state of mitochondrial membrane and exhibits green fluorescence emissions. Briefly, HepG2 cells were seeded into 24-well culture plate at a density of 3×105 cells/750 µl/well and treated with CTP inhibitor, PMCT inhibitor and their combinations for 24 h. Cells were harvested and incubated with JC-1 dye at 37°C and 5% CO2 for 45 min. The disruption of ΔΨm in HepG2 cells was detected by FACSCalibur flow cytometry and the data were analyzed using CellQuset Pro software.

5. Analysis of cell cycle arrest

The effect of citrate transporter inhibitors on cell cycle progression in HepG2 cells were determined using Muse Cell Cycle assay kit (Merck Millipore, Germany). The assay is based on staining cells with PI to analyze DNA contents. Briefly, Cells were seeded in a 35 mm3 disc at 1×106 cells and treated with citrate transporter

inhibitors alone and combinations for 24 h. Then, cells were harvested and fixed with cold 70% ethanol at 4°C at least 12 h. The fixed cells were washed with cold PBS and re-suspended in Muse cell cycle reagent and incubated at room temperature for 30 minutes in the dark. Analysis of cellular DNA s was performed by Muse Cell Analyzer (Merck Millipore, Germany).

6. Determination of DNL protein expression

To determine protein expression in DNL pathway, total protein extraction was performed by M-PER (Mammalian Protein Extraction Reagent) (Thermo Fisher Scientific Inc., Rock ford, IL, USA) following HepG2 cells were treated with combinations of CTP and PMCT inhibitors for 24 h. Extracted protein concentration was quantified by BCA assay (Bicinchoninic acid; Thermo Scientific, Rock ford, IL, USA). Extract proteins were separated by 8% SDS polyacrylamide gel electrophoresis and transferred to polyvinylidene difluoride (PVDF) membranes. The membranes were blocked with Rapid Block Solution (AMRESCO, Solon, OH, USA) for 20 minutes at room temperature and then immunoblotted at 4°C overnight with specific primary antibodies, including anti-fatty acid synthase (FASN; 1:1000) (Abcam, Biomes Diagnostic CO., Ltd, Thailand), anti- Acetyl-CoA carboxylase (ACC; 1:1000) (Merck Millipore, Germany), anti-ATP-citrate lyase (ACLY; 1:1000) and anti-β actin (1:800) (Cell Signaling Technology Inc., USA). Then, immunoblots were incubated with horseradish peroxidase-conjugated goat anti-Rabbit IgG secondary antibody (Life Technologies, invitrogen, NY, USA) 1:5000 in PBST containing 5% skim milk for 2 h at 4°C and followed by visualization with the enhanced chemiluminescence HRP substrate (Luminate Forte, Merck Millipore, Germany). Intensity of protein bands was measured using CCD camera (ImageQuant LAS 4000).

7. Measurement of intracellular citrate level

Cytosolic citrates are substrates for DNL pathway. Conversion of citrate to pyruvate via oxaloacetate was quantified by citrate bioassay kit (C5802: US Biological; Life Sciences, Salem, MA, USA) as described in the manufacturer's protocol. Briefly, HepG2 cells were seeded in 35 mm3 at 1.6×106 cells and incubated with the combinations of citrate transporter inhibitors for 24 h. Subsequently, cells were harvested, homogenized with citrate assay buffer, followed by adding the reaction mix

to each samples. Then, the fluorescence of pyruvate product was measured at Ex/Em 535/590 nm by microplate reader.

8. Measurement of intracellular fatty acid level

To determine intracellular long chain free fatty acid level, a product from DNL pathway, free fatty acid bioAssay kit (F0019-94; US Biological; Life Sciences, Salem, MA, USA) was used as described in the manufacturer's protocol. In the assay, long chain free fatty acids are converted to CoA derivatives, and then oxidized with concomitant generation of fluorescence. Briefly, after incubated with the combinations of citrate transporter inhibitors, HepG2 cells were harvested and homogenized with 1% Triton-X 100 in pure chloroform. The supernatant was air dried to remove chloroform and then dissolved in fatty acid assay buffer. Subsequently, the reaction mix in the assay kit including enzyme mix, enhancer, and fluorescence probe were added and fatty acids were detected by fluorometry at Ex/Em 535/590 nm with microplate reader.

9. Measurement of intracellular triglyceride level

The triglyceride concentration in HepG2 cells after treated with the combinations of citrate transporter inhibitors was determined using triglyceride quantification bioassay kit (T8417; US Biological; Life Sciences, Salem, MA, USA). In the assay, triglycerides converted to free fatty acids and glycerols are oxidized to generate product which is measured by fluorometric method. Briefly, 24 h after treatment, cells were harvested and homogenized with 5% Triton-X-100. The sample was slowly heated from 50°C to 80°C in dry block heater twice times. The supernatant was collected by centrifugation to remove insoluble materials. The lipase and the reaction mix including probe, and assay buffer were added to each sample and incubate for 60 min at room temperature in the dark, followed by detection of the fluorescence at Ex/Em 535/590 nm using microplate reader.

10. Determination of carnitine palmitoyl transferase-1 (CPT-1) activity

CPT-1 activity was quantified by spectrophotometric method as described previously by Kant S., et al (Kant S., Kumar A., & Singh S. M., 2012). Briefly, following combinations of citrate transporter inhibitors treated cells. Mitochondrial proteins were isolated by lysis buffer (Tris-HCl pH 7.4) containing 0.25 mM sucrose and 1 mM EDTA. The samples were centrifuged at 500g at 4°C for 10 min, re-centrifuged at 15,000g at 4°C for 15 min and re-suspended mitochondria pellets in lysis buffer. The

mitochondria protein content was determined. The reaction mix containing Tris-buffer (100 mM, pH 8.0, 0.1% Triton-X-100, 1 mM EDTA), 0.01 mM palmitoyl CoA, and 0.5 mM DTNB were added in each samples followed by measurement O.D. at 412 nm. Then, L-carnitine 1.25 mM was added incubated for 5 min and measured O.D. at 412 nm using microplate reader.

11. Measurement of Bcl2 activation

To determine effect of the combinations of citrate transporter inhibitors on Bcl-2 activity, we measured Bcl-2 phosphorylation relative to total Bcl-2 expression by flow cytometry using Muse Bcl-2 activation dual detection kit (MCH200105; EMD Millipore, Germany). Briefly, cells were seeded in 24-well culture plate at 1.5×105 cells/well and treated with the combinations of citrate transporter inhibitors for 24 h. Then, cells were harvested, fixed in the fixation for 5 min on ice, followed by centrifugation and finally permeabilized cells with the permeabilization buffer for 5 min on ice. The permeabilized cells were mixed in antibodies cocktail (anti-phospho-Bcl-2(Ser70), Alexa Fluor 555, and anti-Bcl-2, PECy5) with 1X assay buffer. Cell samples were then incubated for 30 min at room temperature in the dark, centrifuged at 400g for 5 min at 4°C, re-suspended in 1X assay buffer, and detected Bcl-2 levels by Muse Cell Analyzer (Merck Millipore, Germany).

12. Determination of reactive oxygen species (ROS)

ROS production was assessed using 5-(and-6)-chloromethyl-2', 7'-dichlorodihydrofluorescein diacetate, acetyl ester (C6827; CM-H2DCFDA; Molecular Probe, Thermo Fisher Scientific Inc, MA, USA) an indicator for reactive oxygen species. Intracellular ROS level was detected the converting of H2DCFDA to a DCF that exhibits an orange fluorescence by oxidation and removal of acetate groups by cellular esterases. Briefly, HepG2 cells were seeded in 24-well culture plate at 1.5×105 cells/well for 24h. Cells were treated with citrate transporter inhibitors alone and combinations. After treatment, cells were harvested and re-suspended in PBS containing 10 μM CM-H2DFDA for 30 min at 37°C in the dark. Cells were analyzed by FACSCalibur flow cytometry with CellQuset Pro software.

Data analysis

Compared the result's t test or One-way analysis of variance (ANOVA) with Turkey's post-hoc analysis was used to determine the statistically significant differences among all experimental results. Data will be presented as mean±SEM of at least three independent experiments, $p < 0.05$. All data will be analyzed using the Graph Prism Software version 5.

CHAPTER IV

RESULT

Citrate transporter inhibitors decreased proliferation of HepG2 cells

Treatments of HepG2 cells with CTP and PMCT inhibitors resulted in decreased cell viability as shown in figure 14 A-C. All the inhibitors induced a reduction of the number of viable cells on a dose-dependent manner with IC50 value of 2.5 mM of both CTP inhibitor and PMCT inhibitor treatment alone. The combination of CTP and PMCT showed further cytotoxic effect than CTP or PMCT alone with IC50 of 0.4 mM of each of them. This study suggests that relative lower concentration of combined CTP and PMCT inhibitor promotes anti-proliferative effect compared with either of single compound.

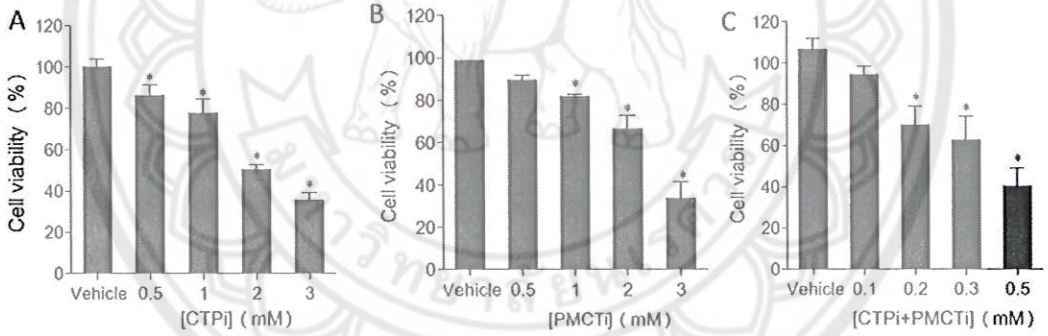

Figure 14 Effect of citrate transporter inhibitors on HepG2 cells. Cells were treated with different concentrations of citrate transporter inhibitors for 24 h, (A) CTP inhibitor (CTPi), (B) PMCT inhibitor (PMCTi), and (C) combination of CTPi and PMCTi. MTT assay was performed and expressed an inhibition as percentage of cell viability compared with 100% of the vehicle control. Three independent experiments were performed for statistical analysis and expressed as mean ± SEM. *denotes statistically significant difference from the vehicle at P<0.05.

Citrate transporter inhibitors induced apoptosis on HepG2 cells

HepG2 cells were treated with citrate transporter inhibitors alone and combination at IC50 concentrations obtained from MTT result for 24 h. Cell death with apoptosis was then detected by annexin V/PI staining and measured by flow cytometry. The results showed in figure 15, all single therapy of 2.5 mM citrate transporter inhibitors significantly reduced viability of cells to 57-66% and increased a apoptotic cell death rate to 34% compared to the control where apoptotic cells was 6%. The combination of CTP and PMCT inhibitors at 0.4 mM of each showed similar apoptotic induction effect observed from single inhibitor on enhanced rate of apoptosis to 39%. Thus, combination with lower concentrations of CTP inhibitor plus PMCT inhibitors than inhibitor alone exhibited potent apoptotic induction.

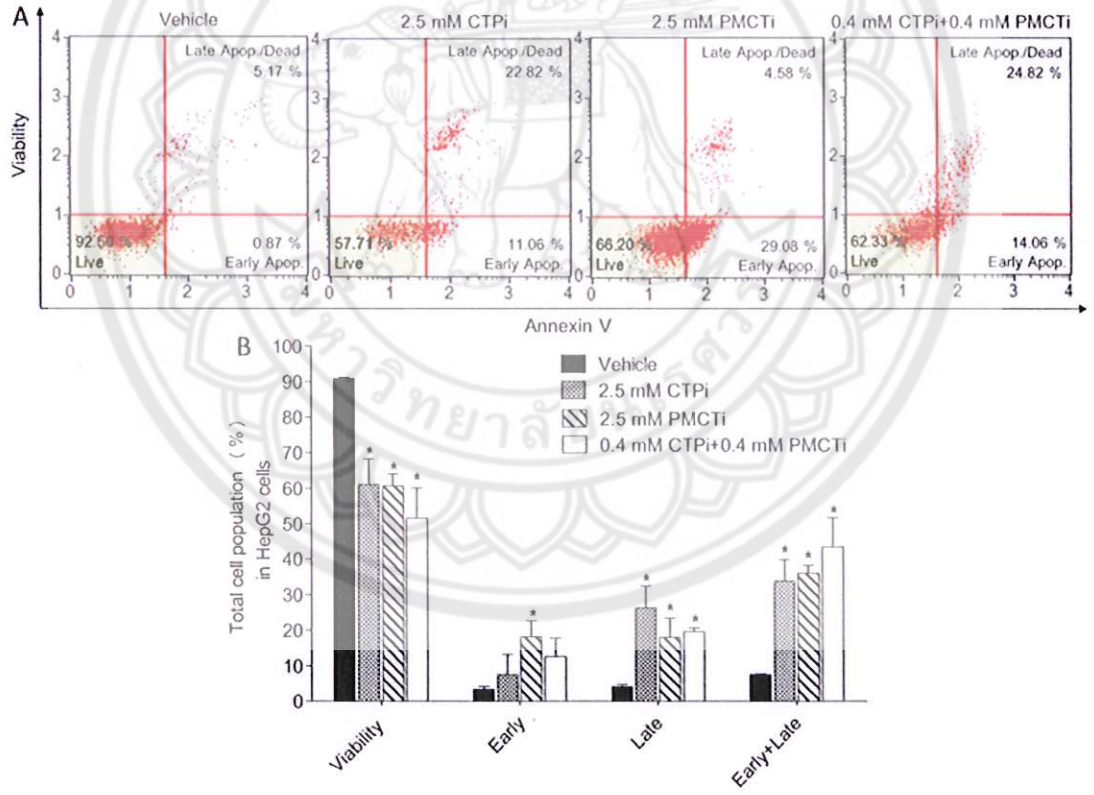

Figure 15 Effect of citrate transporter inhibitors on apoptosis of HepG2 cells. Cells were treated with IC50 concentrations of citrate transporter inhibitors alone and combination for 24 h, double stained with annexin V/ PI, and defected by flow cytometry. The control was defined as vehicle that cells were treated with media containing 0.2% DMSO alone. (A) Flow cytometry showed representative dot

plot analysis. (B) Effect of citrate transporter inhibitors on apoptosis of HepG2 cells represent in bar graph. All data were mean ± SEM of at least three independent experiments.* P<0.05 versus control group.

Citrate transporter inhibitors promoted loss of ΔΨm in HepG2 cells

JC-1 staining was performed to investigate effect of citrate transporter inhibitor on induction of apoptosis through loss of ΔΨm. As shown in figure 16. Cells treated with citrate transporter inhibitors alone showed a loss of ΔΨm to 51.8% and 44.8% following 24 h incubation with 2.5 mM CTP inhibitor and 2.5 mM PMCT inhibitor alone, respectively. Combination of CTP inhibitor and PMCT inhibitor at 0.4 mM of each for 24 h exhibited more potent effect on enhanced loss of ΔΨm to 55.7% compared to 8.8% of the control. These results suggest that citrate transporter inhibitors exert mitochondrial dependent apoptotic induction in HepG2 cells.

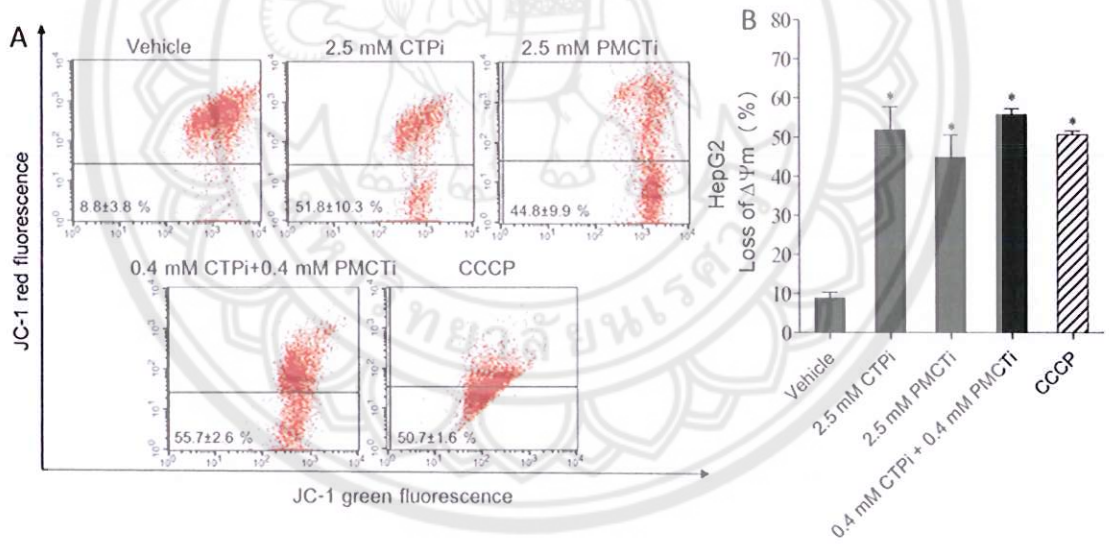

Figure 16 Effect of citrate transporter inhibitors on mitochondria membrane potential (ΔΨm) of HepG2 cells. After 24 h, cells were incubated with single and combinations of citrate transporter inhibitors with IC50 concentrations. (A) The ΔΨm was detected by flow cytometry and shown in representative dot plot analysis. (B) Percentage of the loss of ΔΨm was shown in bar graph. All data were mean ± SEM of at least three independent experiments. * P<0.05 versus control group.

Citrate transporter inhibitors exhibited cell cycle arrest in HepG2 cells

To investigate cell cycle progression during apoptosis, HepG2 cells were treated with citrate transporter inhibitors alone and combinations. After 24 h, treated cells were detected their population in each phases of cell cycle. As shown in figure 17, CTP inhibitor, PMCT inhibitor, and combination of CTP and PMCT inhibitors treated cells caused the cell cycle arrest in S and G2/M phases with reduction of cells in G0/G1 phase to 44%, 42% and 49%, respectively compared with 60% of the vehicle. Cell cycle arrest supports apoptotic induction effect of citrate transporter inhibitors in HeG2 cells.

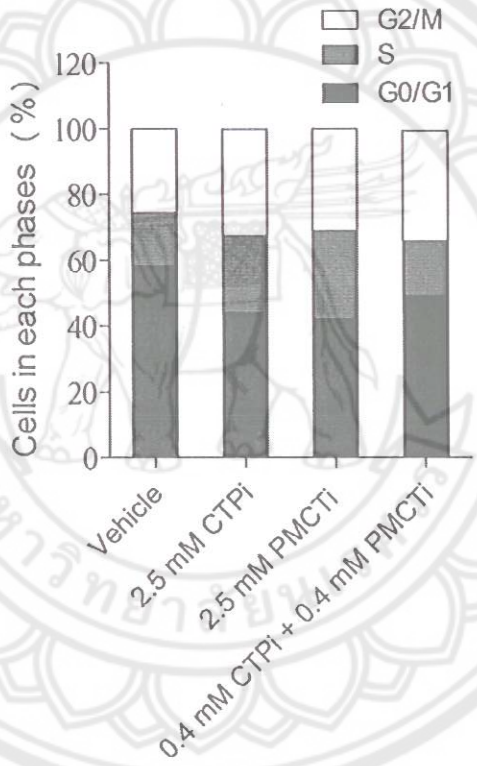

Figure 17 Effect of citrate transporter inhibitors on cell cycle arrest. After 24 h, cells were incubated with single and combinations of citrate transporter inhibitors with IC50 concentrations. The bar charts showed percentages of cells population in G0/G1, S, and G2/M phrases (set as 100%). The control was defined as vehicle that cells were treated with media containing 0.2% DMSO alone. Data from at least three dependent experiments were expressed as mean±SEM, n=3,*p < 0.05.

Combination of citrate transporter inhibitors decreased citrate, fatty acid, and triglyceride levels but did not affect lipogenic protein expression in HepG2 cells

We further investigated decreased of fatty acid levels in DNL pathway following inhibition of citrate transport could potentially exert apoptotic induction in HepG2 cells. Reduction of fatty acid synthesis is known to cause apoptosis in cancer cells (Fan H., et al., 2016; Puig T., Relat J., et al., 2008). The expression of proteins in DNL pathway was investigated by immunoblot analysis. After cells were treated with combinations of CTP and PMCT inhibitors for 24 h, the expression of proteins including FASN, ACC, and ACLY did not alter as shown in figure 18. Thus, combination of CTP and PMCT inhibitors in HepG2 has no effect on DNL lipogenic protein expression in HepG2 cells. However, combination of CTP and PMCT inhibitors decreased intracellular citrate, fatty acid, and triglyceride to 47%, 40%, and 51% respectively compared to 100% of the vehicle. These results demonstrate combination of CTP and PMCT inhibitors causes marked suppression of DNL pathway in HepG2 cells.

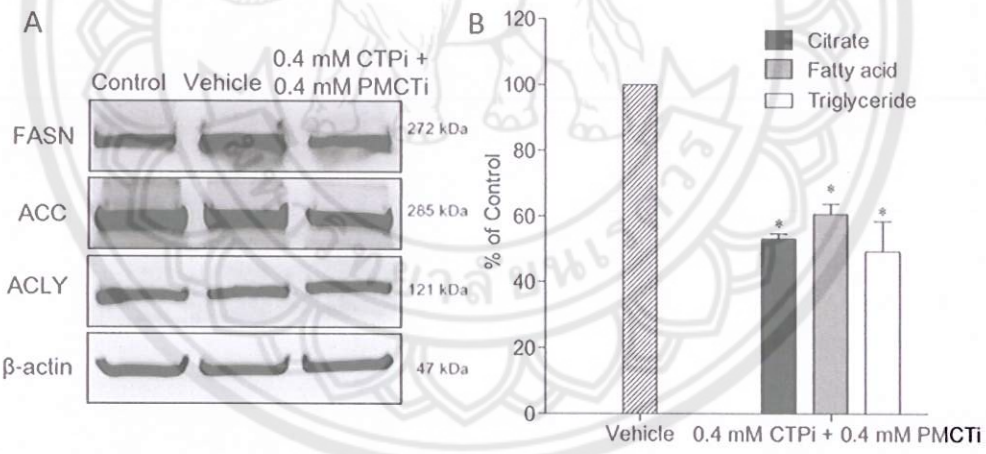

Figure 18 Effect of combinations of CTP and PMCT inhibitors on expression of lipogenic protein, intracellular citrate, fatty acid, and triglyceridelevels. HepG2 cells were treated with combination of CTP and PMCT inhibitors at 0.4 mM concentrations of each for 24 h. Cell exposed to 0.2% DMSO was set as vehicle. Equal amount of total protein extracts was subjected to immunoblotting assay to detect expression of FASN, ACC, and ACLY proteins. β-actin was used to normalize equal amount and intensity of protein bands. (A) Immunoblot was visualized using a CCD camera. (B) Intracellular citrate, fatty acid, and triglyceride levels were quantified as described in materials and methods. The result showed mean± SEM, n=3, *p < 0.05 from three independent experiments

Suppression of CPT-1 activity contributed to combinations of citrate transporter inhibitors inducing apoptosis in HepG2 cells

We further investigated an accumulation of malonyl-CoA mediated by depletion of fatty acid synthesis became one of major contributors to apoptotic induction by citrate transporter inhibitor (Puig T., Vazquez-Martin A., et al., 2008; Thupari J. N., Pinn M. L., & Kuhajda F. P., 2001). Fatty acid levels of DNL pathway is known to exert negative inhibitory effect on ACC activity that leads to alteration of malonyl CoA synthesis, which in turn regulates CPT-1 activity (Dobrzyn P., et al., 2004; Huang H., et al., 2013). HepG2 cells exhibited a loss of $\Delta\Psi m$ 9.5% after applied TOFA alone to inhibit ACC activity, as shown in figure 19A. Combination of citrate transporter inhibitors and pretreated TOFA and citrate transporter inhibitors combination for 24 h also induced damage of $\Delta\Psi m$ approximately 50 % compared to 8-9 % of vehicle, suggesting apoptosis induction by combination of citrate transporter inhibitors was not relieved following pretreated cells with TOFA. Additional supporting evidence shown in figure 19B found that in combination of citrate transporter inhibitors reduced CPT-1 activity by 30% compared to the control. Taken together, these data suggest that when inhibited citrate transport, depletion of fatty acid synthesis and down regulates CPT-1 activity predominantly enhances apoptosis in HepG2 cells. Meanwhile, the same finding with previous reports (Wang C., et al., 2009; Zhou W., et al., 2007) was found in the present experiment that TOFA did not restore apoptotic cells from cytotoxic effect of C75. This was due to C75 exhibited up regulation of CPT-1 activity, suggesting an adverse effect of C75.

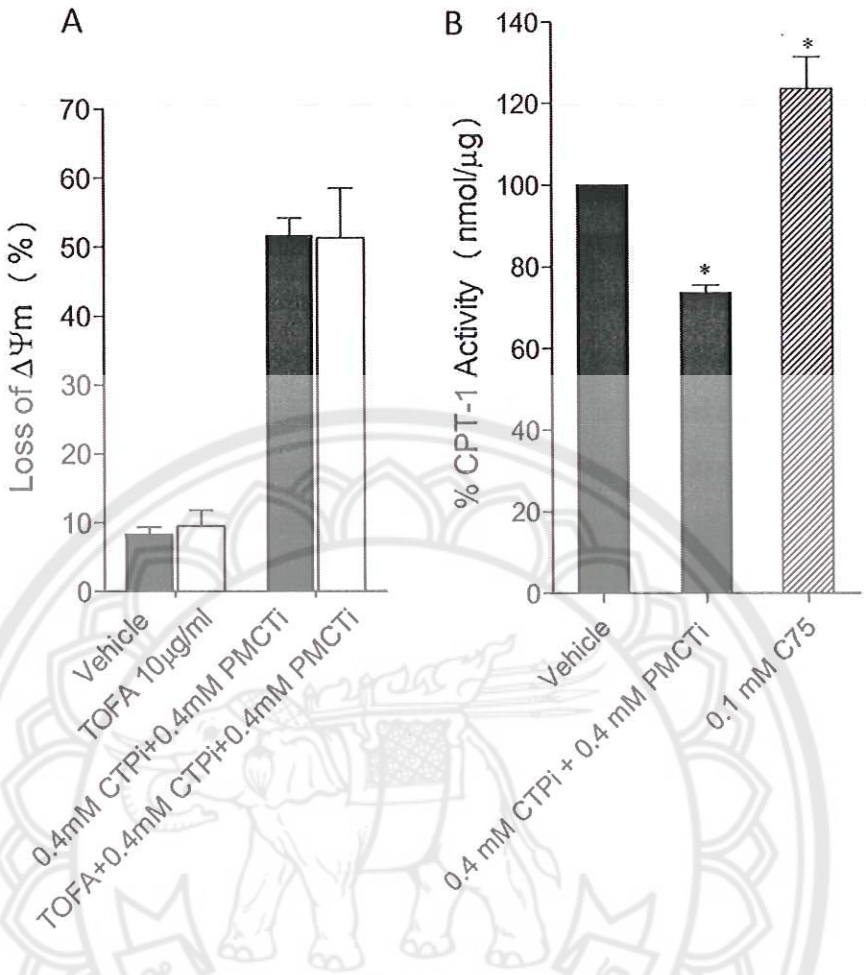

Figure 19 Effect of combination of citrate transporter inhibitors on activity of CPT-1

(A) The loss of ΔΨm was determined by JC-1 staining and detected by flow cytometry. Cells were treated with 10 μg/ml of TOFA for 24 h, pretreated with 10 μg/ml of TOFA for 1 h followed by treated with combination of CTP and PMCT inhibitor at 0.4 mM of each. (B) Percentage of CPT-1 activity was determined in cells treated with combination of CTP and PMCT inhibitor at 0.4 mM of each or 0.1 mM of C75 for 24 h. The vehicle was set as control cells treated with 0.2% DMSO. Data were presented as mean± SEM of three independent experiments, n=3,*p < 0.05.

Combination of citrate transporter inhibitors induced intracellular ROS generation and decreased Bcl-2 activity in HepG2 cells.

Increased intracellular generation of ROS could lead to apoptosis in cancers (Ling Y. H., Liebes L., Zou Y., & Perez-Soler R., 2003; Liou G. Y. & Storz P., 2010). The present experiment investigated apoptotic induction by citrate transporter inhibitors involved an elevating of ROS formation. The fluorescence DCF product of CM-H2DCFDA was used to determine intracellular ROS levels following treatment with citrate transporter inhibitors for 24 h. As shown in figure 20A, there was significant increase of ROS product level in cells treated with combination of CTP and PMCT inhibitors at 0.4 mM concentration of each compared to control. HepG2 cells exhibited a loss of $\Delta\Psi m$ 14% after treated NAC alone to inhibit ROS production, as shown in figure 20B. Combination of citrate transporter inhibitors and pretreated with NAC for 2 h also reduced damage of $\Delta\Psi m$ approximately 30 % compared to 9 % of vehicle, suggesting apoptosis induction by combination of citrate transporter inhibitors was relieved following pretreated cells with NAC. Thus, these results suggest that combinations of CTP and PMCT inhibitors induced apoptosis are dependent of ROS generation.

After 24 h of incubating HepG2 cells with citrate transporter inhibitors in combinations, Bcl-2 activity was measured. As shown in figure 20C, we found significant alteration of Bcl-2 activity between vehicle and treated cells decreased by approximately 55% compared to 100% of control. Thus, when applied citrate transporter inhibitors in combination induces apoptosis through the intrinsic apoptotic pathway via suppression of Bcl-2 activity in HepG2 cells.

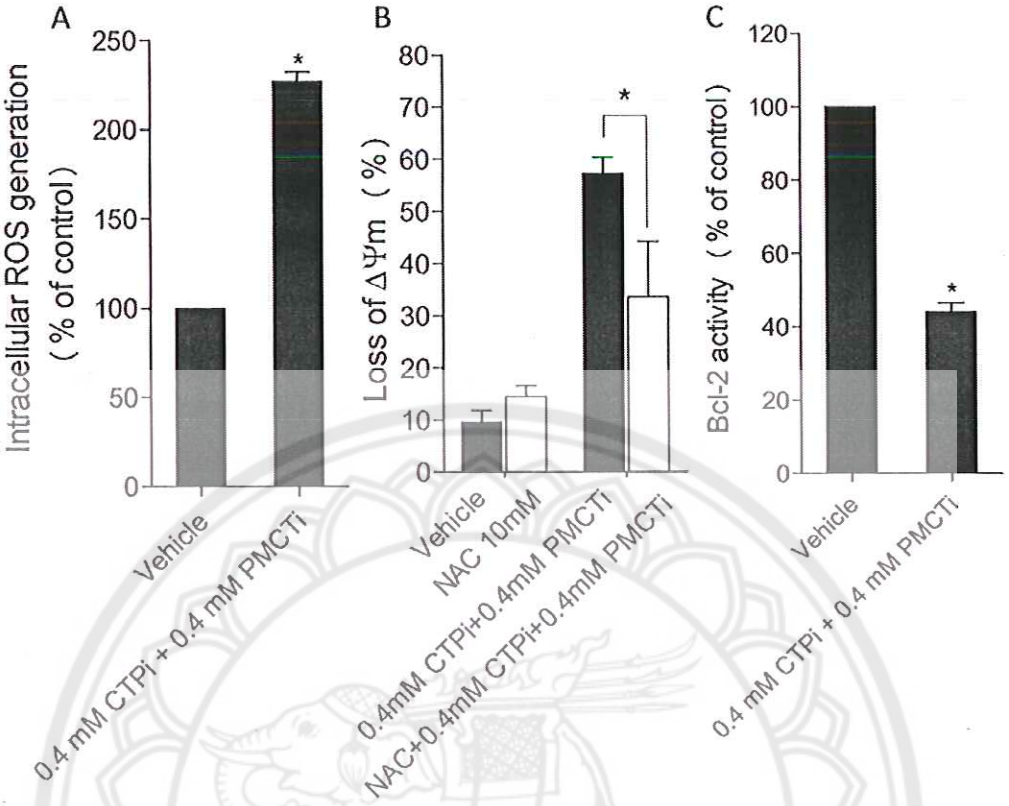

Figure 20 Effect of citrate transporter inhibitor combinations on apoptosis pathways and ROS generation in HepG2 cells. Cells were treated with combination of CTP and PMCT inhibitors at 0.4 mM of each for 24 h. (A) Intracellular ROS production was measured using flow cytometry. (B) Cells were treated with 10 mM of NAC for 24 h, pretreated with 10 mM of NAC for 2 h followed by treated with combination of CTP and PMCT inhibitor at 0.4 mM of each. (C) Bcl-2 activity was quantified by flow cytometry using Bcl-2 phosphorylation relative to total Bcl-2 expression levels compared to 100% of vehicle. Data were presented as mean±SD, n=3 from at least three independent experiments, *p < 0.05.

CHAPTER V

DISCUSSION AND CONCLUSION

The combination of CTP and PMCT inhibitors resulted in abrogation of fatty acid production of DNL pathway, which led to augmentation mitochondrial-dependent apoptosis in HepG2 cells. In response to DNL inhibition, suppressed CPT-1 activity as a consequence of an accumulation of malonyl-CoA accounted for increased cytotoxic and apoptosis. The present study also showed concomitant enhanced ROS generation secondary to decreased fatty acid production which resulted in abrogation of proliferation and activation of apoptosis in cancer cells. Moreover, HepG2 cells exposure to combination of CTP and PMCT inhibitors also induced cell cycle arrest at G2/M phase.

The present study examined the expression of lipogenic enzymes in DNL pathway including FASN, ACC, and ACLY. Our results showed that the expression of lipogenic enzymes were not altered following combination treatment. This suggesting citrate transporter inhibition induced apoptosis in HepG2 cells is not related to the expression of lipogenic enzymes in DNL pathway. However, the activity of the enzyme in this pathway measured by intracellular fatty acids and triglycerides; substrate and product of DNL pathway, were reduced (Escriba P. V., et al., 2015). We suggest that inhibition of DNL by citrate transporter inhibitors causes an apoptosis in HepG2 cells.

It has been reported that blockade of FASN leads to apoptosis in human breast cancer (Thupari J. N., et al., 2001) and in vivo after EGCG treatment (epigallocatechin-3-gallate) (Puig T., Vazquez-Martin A., et al., 2008). The effect of siRNA-mediated knockdown of ACC-α on prostate cancer cells induces growth arrest and tumor cell death (Brusselmans K., De Schrijver E., Verhoeven G., & Swinnen J. V., 2005). Inhibition of ACLY causes the growth suppression of cancer cells (Migita T., et al., 2014). The previous study has reported that decreased fatty acids and triglycerides induce alteration of lipid composition that switches the cancer cells from proliferation to quiescent state (Escriba P. V., et al., 2015).

Enhanced ROS generation has been recognized as one of causes of apoptosis (Ling Y. H., et al., 2003). In the present study, we found that citrate transporters inhibitor-induced apoptosis through the loss of $\Delta\Psi m$ was related to an increased ROS level. We suggest that combination of CTP and PMCT inhibitors induced apoptosis is depending on ROS generation. Inhibition of citrate transported from mitochondrial TCA cycle into cytoplasm results in an accumulation of citrate in mitochondria. The intra-mitochondrial citrate directly inhibits succinate dehydrogenase (SDH), complex II, succinate-ubiquinone oxidoreductase, a tetrameric iron-sulfur flavoprotein of the inner mitochondrial membrane that acts as the catalyzer of conversion of succinate into fumarate. Impaired electron transport as a result of SDH inhibition promotes a substantial amount of ROS production leading to an increase of oxidative stress and apoptosis (Hillar M., Lott V., & Lennox B., 1975; Iacobazzi V. & Infantino V., 2014; Zorov D. B., Juhaszova M., & Sollott S. J., 2014).

In addition to LCFA, sphingolipids such as ceramide and sphingosine-1-phosphate (S1P) are generated from DNL pathway. Sphingolipids are synthesized from the condensation of palmitate which is one of the most LCFA production and serine to form dihydrosphingosine. Then dihydrosphingosine is transformed to dihydroceramide followed by (dihydro)-ceramide synthase activity. Ceramide is finally generated from dihydroceramide by the action of desaturase enzyme. Moreover, ceramide can be converted to other interconnected bioactive lipid species, especially S1P by sphingosine kinase (SphKs) (Hannun Y. A. & Obeid L. M., 2008). Furthermore, balancing roles between sphingolipids, ceramide, and S1P is required for cell function and survival. It has been reported that ceramide induces apoptosis in cancer cells while S1P functions as a survival factor in various cells (Oskouian B. & Saba J. D., 2010). The current evidence has demonstrated that anti-apoptotic Bcl-2 reduces ceramide accumulation and mitochondrial permeability transition pore opening, as well as increases intracellular S1P levels by stimulates the expression and activity of SphK1, thereby decreasing ceramide/S1P ratio (Bektas M., et al., 2005). In addition, Bcl-2 affects the enzymes involved in ceramide metabolisms such as ceramide synthases and sphingomyelinases, leading to reduction of apoptosis and increase of cell survival (Beverly L. J., et al., 2013; Sawada M., et al., 2000). The present study found that citrate transporter inhibitors caused suppression of Bcl-2 activity. Thus, we suggest that apoptosis is triggered by

enhanced ceramide accumulation as a consequence of suppression of Bcl-2 activity in HepG2 cells.

Previous report suggested that transcriptional factor PPARα is one of the regulators of CPT-1 expression. Depletion of ACLY or LCFAs reported as suppressors of PPARα activity (Migita T., et al., 2014). Thus, in our study, suppression of LCFA as a result of citrate transporter inhibitors could inhibit PPARα activity that consequently leads to reduction of CPT-1 activity. This leads to suppression the delivery rate of LCFAs into mitochondria. Finally, LCFAs accumulation from this suppression is stimulated into ceramide production (Aon M. A., Bhatt N., & Cortassa S. C., 2014; Roden M., 2005). The present study found that applied combination of citrate transporter inhibitors showed downregulation of CPT-1 activity. We speculate a suppression of PPARα following DNL inhibition. The finalized downregulation of CPT-1 activity from these sequence events augments the depression of catalization and transferration of LCFAs for fatty acid β-oxidation process. Herein, accumulation of LCFAs can be converted to ceramide which causes cellular consequence of apoptosis. The capable of ceramide accumulation-induced apoptosis in cancer cells has been reported to involve expressions of pro-apoptotic genes BNIP3, tumor necrosis factor related apoptosis-inducing ligand (TRAIL), and death-associated protein kinase 2 (DAPK2) (Bandyopadhyay S., et al., 2006).

In conclusion, our findings demonstrate that the combination of CTP and PMCT inhibitor will potentially the development of a novel anti-cancer therapy that targets on the inhibition of the DNL for HCC and other cancers. The further suggestion of this research that will be the ability to selectively inhibit DNL pathway may be a novel therapeutic of metabolic disorders, including human obesity, hyperlipidemia, hypercholesterolemia, and type 2 diabetes. All of these diseases are known to associate with the synthesis of excess lipid, cholesterol, and glucose.

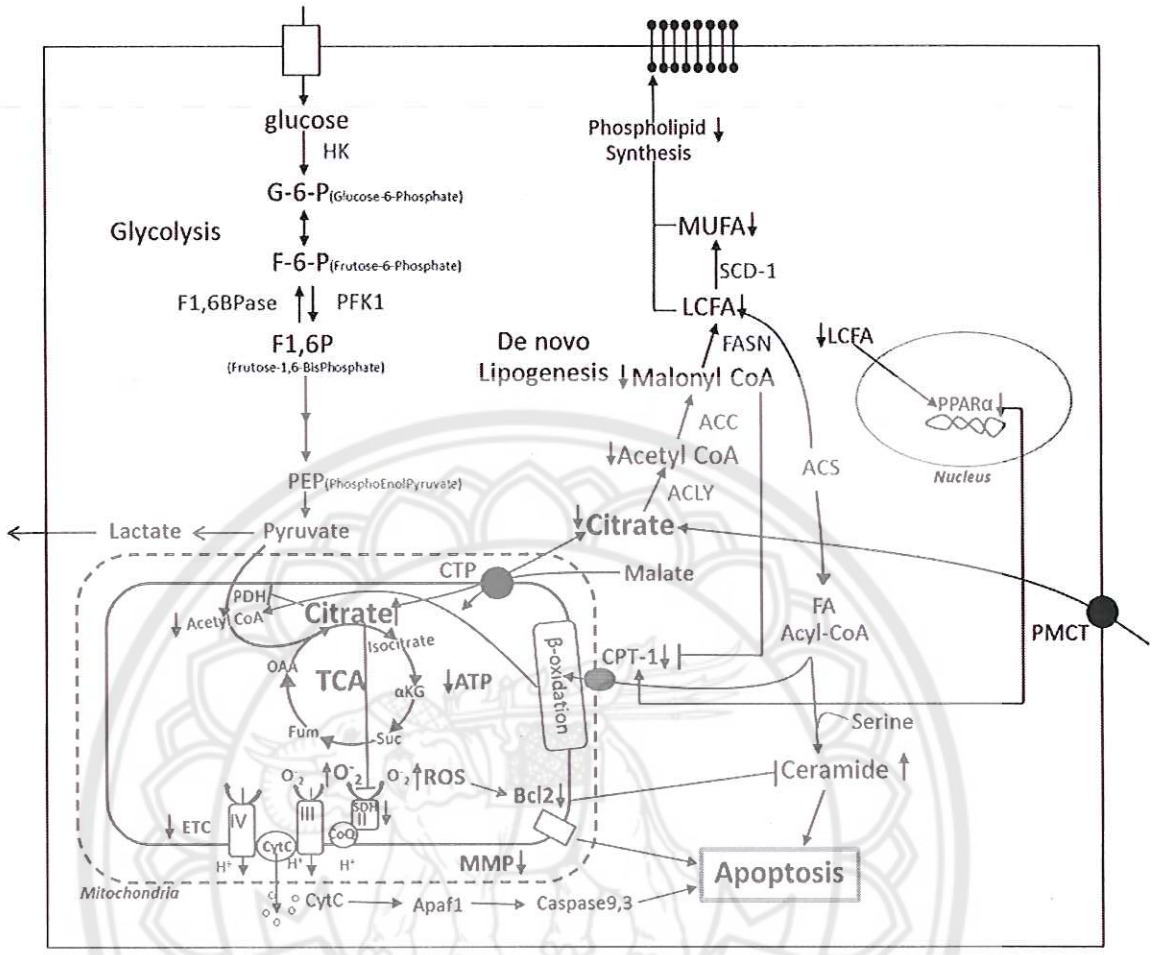

Figure 21 The proposed mechanism of apoptosis induction and inhibit cell viability by combination of CTP and PMCT inhibitor in HepG2 cells

CTP; citrate transport protein, PMCT; plasma membrane citrate transporter, MMP; mitochondrial membrane potential, CytC; Cytochrome C, PDH; Pyruvate dehydrogenase, SDH; Succinate dehydrogenase, ETC; Electron transport chain, GF; Growth factor, RTK; Receptor tyrosine kinase, SCD; stearoyl-CoA desaturase, ACS; Acyl-CoA synthetase, AMPK; Activation of AMP-activated protein kinase, CPT-1; Carnitine palmitoyltransferase I, ACC; Acetyl-CoA carboxylase, ACLY; ATP citrate lyase, FASN; Fatty acid synthase, SREBP1; Sterol regulatory element-binding protein, MUFA; Monounsaturated fatty acid, LCFA; long chain fatty acids.

REFERENCES

REFERENCES

Ahsan M. K., Okuyama H., Hoshino Y., Oka S., Masutani H., Yodoi J., & Nakamura H. (2009). Thioredoxin-binding protein-2 deficiency enhances methionine-choline deficient diet-induced hepatic steatosis but inhibits steatohepatitis in mice. *Antioxid Redox Signal, 11*(10), 2573-2584. doi:10.1089/ars.2009.2385

Ameer F., Scandiuzzi L., Hasnain S., Kalbacher H., & Zaidi N. (2014). De novo lipogenesis in health and disease. *Metabolism, 63*(7), 895-902. doi:10.1016/j.metabol.2014.04.003

Aon M. A., Bhatt N., & Cortassa S. C. (2014). Mitochondrial and cellular mechanisms for managing lipid excess. *Frontiers in Physiology, 5*, 282. doi:10.3389/fphys.2014.00282

Ashkenazi A. (2008). Directing cancer cells to self-destruct with pro-apoptotic receptor agonists. *Nat Rev Drug Discov, 7*(12), 1001-1012. doi:10.1038/nrd2637

Bandyopadhyay S., Zhan R., Wang Y., Pai S. K., Hirota S., Hosobe S., & Watabe K. (2006). Mechanism of apoptosis induced by the inhibition of fatty acid synthase in breast cancer cells. *Cancer Res, 66*(11), 5934-5940. doi:10.1158/0008-5472.can-05-3197

Bektas M., Jolly P. S., Muller C., Eberle J., Spiegel S., & Geilen C. C. (2005). Sphingosine kinase activity counteracts ceramide-mediated cell death in human melanoma cells: role of Bcl-2 expression. *Oncogene, 24*(1), 178-187. doi:10.1038/sj.onc.1208019

Beverly L. J., Howell L. A., Hernandez-Corbacho M., Casson L., Chipuk J. E., & Siskind L. J. (2013). BAK activation is necessary and sufficient to drive ceramide synthase-dependent ceramide accumulation following inhibition of BCL2-like proteins. *Biochem J, 452*(1), 111-119. doi:10.1042/bj20130147

Brusselmans K., De Schrijver E., Verhoeven G., & Swinnen J. V. (2005). RNA interference-mediated silencing of the acetyl-CoA-carboxylase-alpha gene induces growth inhibition and apoptosis of prostate cancer cells. *Cancer Res, 65*(15), 6719-6725. doi:10.1158/0008-5472.can-05-0571

Caporossi D., Ciafre S. A., Pittaluga M., Savini I., & Farace M. G. (2003). Cellular responses to H(2)O(2) and bleomycin-induced oxidative stress in L6C5 rat myoblasts. *Free Radic Biol Med, 35*(11), 1355-1364.

Currie E., Schulze A., Zechner R., Walther T. C., & Farese R. V., Jr. (2013). Cellular fatty acid metabolism and cancer. *Cell Metab, 18*(2), 153-161. doi:10.1016/j.cmet.2013.05.017

Diraison F., Yankah V., Letexier D., Dusserre E., Jones P., & Beylot M. (2003). Differences in the regulation of adipose tissue and liver lipogenesis by carbohydrates in humans. *J Lipid Res, 44*(4), 846-853. doi:10.1194/jlr.M200461-JLR200

Dobrzyn P., Dobrzyn A., Miyazaki M., Cohen P., Asilmaz E., Hardie D. G., & Ntambi J. M. (2004). Stearoyl-CoA desaturase 1 deficiency increases fatty acid oxidation by activating AMP-activated protein kinase in liver. *Proc Natl Acad Sci U S A, 101*(17), 6409-6414. doi:10.1073/pnas.0401627101

Droge W. (2002). Free radicals in the physiological control of cell function. *Physiol Rev, 82*(1), 47-95. doi:10.1152/physrev.00018.2001

Effert P. J., Bares R., Handt S., Wolff J. M., Bull U., & Jakse G. (1996). Metabolic imaging of untreated prostate cancer by positron emission tomography with 18fluorine-labeled deoxyglucose. *J Urol, 155*(3), 994-998.

Escriba P. V., Busquets X., Inokuchi J., Balogh G., Torok Z., Horvath I., & Vigh L. (2015). Membrane lipid therapy: Modulation of the cell membrane composition and structure as a molecular base for drug discovery and new disease treatment. *Prog Lipid Res, 59*, 38-53. doi:10.1016/j.plipres.2015.04.003

Fan H., Liang Y., Jiang B., Li X., Xun H., Sun J., & Ma X. (2016). Curcumin inhibits intracellular fatty acid synthase and induces apoptosis in human breast cancer MDA-MB-231 cells. *Oncol Rep, 35*(5), 2651-2656. doi:10.3892/or.2016.4682

Gaggini M., Morelli M., Buzzigoli E., DeFronzo R. A., Bugianesi E., & Gastaldelli A. (2013). Non-alcoholic fatty liver disease (NAFLD) and its connection with insulin resistance, dyslipidemia, atherosclerosis and coronary heart disease. *Nutrients, 5*(5), 1544-1560. doi:10.3390/nu5051544

Hannun Y. A., & Obeid L. M. (2008). Principles of bioactive lipid signalling: lessons from sphingolipids. *Nat Rev Mol Cell Biol, 9*(2), 139-150. doi:10.1038/nrm2329

Hillar M., Lott V., & Lennox B. (1975). Correlation of the effects of citric acid cycle metabolites on succinate oxidation by rat liver mitochondria and submitochondrial particles. *J Bioenerg, 7*(1), 1-16.

Huang H., McIntosh A. L., Martin G. G., Petrescu A. D., Landrock K. K., Landrock D., & Schroeder F. (2013). Inhibitors of Fatty Acid Synthesis Induce PPAR alpha -Regulated Fatty Acid beta -Oxidative Genes: Synergistic Roles of L-FABP and Glucose. *PPAR Res, 2013*, 865604. doi:10.1155/2013/865604

Iacobazzi V., & Infantino V. (2014). Citrate--new functions for an old metabolite. *Biol Chem, 395*(4), 387-399. doi:10.1515/hsz-2013-0271

Impheng H., Pongcharoen S., Richert L., Pekthong D., & Srisawang P. (2014). The selective target of capsaicin on FASN expression and de novo fatty acid synthesis mediated through ROS generation triggers apoptosis in HepG2 cells. *PLoS One, 9*(9), e107842. doi:10.1371/journal.pone.0107842

Jozwiak P., Forma E., Brys M., & Krzeslak A. (2014). O-GlcNAcylation and Metabolic Reprograming in Cancer. *Front Endocrinol (Lausanne), 5*, 145. doi:10.3389/fendo.2014.00145

Kant S., Kumar A., & Singh S. M. (2012). Fatty acid synthase inhibitor orlistat induces apoptosis in T cell lymphoma: role of cell survival regulatory molecules. *Biochim Biophys Acta, 1820*(11), 1764-1773. doi:10.1016/j.bbagen.2012.07.010

Kato Y., Lambert C. A., Colige A. C., Mineur P., Noel A., Frankenne F., & Tsukuda M. (2005). Acidic extracellular pH induces matrix metalloproteinase-9 expression in mouse metastatic melanoma cells through the phospholipase D-mitogen-activated protein kinase signaling. *J Biol Chem, 280*(12), 10938-10944. doi:10.1074/jbc.M411313200

Kim J. U., Shariff M. I., Crossey M. M., Gomez-Romero M., Holmes E., Cox I. J., & Taylor-Robinson S. D. (2016). Hepatocellular carcinoma: Review of disease and tumor biomarkers. *World J Hepatol, 8*(10), 471-484. doi:10.4254/wjh.v8.i10.471

Klingenberg M. (1972). Kinetic study of the tricarboxylate carrier in rat liver mitochondria. *Eur J Biochem, 26*(4), 587-594.

Kolukula V. K., Sahu G., Wellstein A., Rodriguez O. C., Preet A., Iacobazzi V., & Avantaggiati M. L. (2014). SLC25A1, or CIC, is a novel transcriptional target of mutant p53 and a negative tumor prognostic marker. *Oncotarget, 5*(5), 1212-1225.

Kowaltowski A. J., de Souza-Pinto N. C., Castilho R. F., & Vercesi A. E. (2009). Mitochondria and reactive oxygen species. *Free Radic Biol Med, 47*(4), 333-343. doi:10.1016/j.freeradbiomed.2009.05.004

Ling Y. H., Liebes L., Zou Y., & Perez-Soler R. (2003). Reactive oxygen species generation and mitochondrial dysfunction in the apoptotic response to Bortezomib, a novel proteasome inhibitor, in human H460 non-small cell lung cancer cells. *J Biol Chem, 278*(36), 33714-33723. doi:10.1074/jbc.M302559200

Liou G. Y., & Storz P. (2010). Reactive oxygen species in cancer. *Free Radic Res, 44*(5), 479-496. doi:10.3109/10715761003667554

Liu Y., Zuckier L. S., & Ghesani N. V. (2010). Dominant uptake of fatty acid over glucose by prostate cells: a potential new diagnostic and therapeutic approach. *Anticancer Res, 30*(2), 369-374.

Lu J., Tan M., & Cai Q. (2015). The Warburg effect in tumor progression: Mitochondrial oxidative metabolism as an anti-metastasis mechanism. *Cancer Lett, 356*(2 Pt A), 156-164. doi:10.1016/j.canlet.2014.04.001

Lunt S. Y., & Vander Heiden M. G. (2011). Aerobic glycolysis: meeting the metabolic requirements of cell proliferation. *Annu Rev Cell Dev Biol, 27*, 441-464. doi:10.1146/annurev-cellbio-092910-154237

Martindale J. L., & Holbrook N. J. (2002). Cellular response to oxidative stress: Signaling for suicide and survival. *J Cell Physiol, 192*(1), 1-15. doi:10.1002/jcp.10119

Martinez-Outschoorn U. E., Prisco M., Ertel A., Tsirigos A., Lin Z., Pavlides S., & Lisanti M. P. (2011). Ketones and lactate increase cancer cell "stemness," driving recurrence, metastasis and poor clinical outcome in breast cancer: achieving personalized medicine via Metabolo-Genomics. *Cell Cycle, 10*(8), 1271-1286. doi:10.4161/cc.10.8.15330

Mashima T., Seimiya H., & Tsuruo T. (2009). De novo fatty-acid synthesis and related pathways as molecular targets for cancer therapy. *Br J Cancer, 100*(9), 1369-1372. doi:10.1038/sj.bjc.6605007

Menendez J. A., & Lupu R. (2007). Fatty acid synthase and the lipogenic phenotype in cancer pathogenesis. *Nat Rev Cancer, 7*(10), 763-777. doi:10.1038/nrc2222

Migita T., Okabe S., Ikeda K., Igarashi S., Sugawara S., Tomida A., & Seimiya H. (2014). Inhibition of ATP citrate lyase induces triglyceride accumulation with altered fatty acid composition in cancer cells. *Int J Cancer, 135*(1), 37-47. doi:10.1002/ijc.28652

Ohki T., Tateishi R., Shiina S., Goto E., Sato T., Nakagawa H., & Omata M. (2009). Visceral fat accumulation is an independent risk factor for hepatocellular carcinoma recurrence after curative treatment in patients with suspected NASH. *Gut, 58*(6), 839-844. doi:10.1136/gut.2008.164053

Oskouian B., & Saba J. D. (2010). Cancer Treatment Strategies Targeting Sphingolipid Metabolism. *Advances in experimental medicine and biology, 688*, 185-205.

Park E. J., Lee J. H., Yu G. Y., He G., Ali S. R., Holzer R. G., & Karin M. (2010). Dietary and genetic obesity promote liver inflammation and tumorigenesis by enhancing IL-6 and TNF expression. *Cell, 140*(2), 197-208. doi:10.1016/j.cell.2009.12.052

Paschos P., & Paletas K. (2009). Non alcoholic fatty liver disease and metabolic syndrome. *Hippokratia, 13*(1), 9-19.

Puig T., Relat J., Marrero P. F., Haro D., Brunet J., & Colomer R. (2008). Green tea catechin inhibits fatty acid synthase without stimulating carnitine palmitoyltransferase-1 or inducing weight loss in experimental animals. *Anticancer Res, 28*(6a), 3671-3676.

Puig T., Vazquez-Martin A., Relat J., Petriz J., Menendez J. A., Porta R., & Colomer R. (2008). Fatty acid metabolism in breast cancer cells: differential inhibitory effects of epigallocatechin gallate (EGCG) and C75. *Breast Cancer Res Treat, 109*(3), 471-479. doi:10.1007/s10549-007-9678-5

Rahman R., Hammoud G. M., Almashhrawi A. A., Ahmed K. T., & Ibdah J. A. (2013). Primary hepatocellular carcinoma and metabolic syndrome: An update. *World Journal of Gastrointestinal Oncology, 5*(9), 186-194. doi:10.4251/wjgo.v5.i9.186

Ren J., Xiao Y. J., Singh L. S., Zhao X., Zhao Z., Feng L., & Xu Y. (2006). Lysophosphatidic acid is constitutively produced by human peritoneal mesothelial cells and enhances adhesion, migration, and invasion of ovarian cancer cells. *Cancer Res, 66*(6), 3006-3014. doi:10.1158/0008-5472.can-05-1292

Robinson B. H., Williams G. R., Halperin M. L., & Leznoff C. C. (1971). Factors affecting the kinetics and equilibrium of exchange reactions of the citrate-transporting system of rat liver mitochondria. *J Biol Chem, 246*(17), 5280-5286.

Roden M. (2005). Muscle triglycerides and mitochondrial function: possible mechanisms for the development of type 2 diabetes. *Int J Obes (Lond), 29 Suppl 2*, S111-115.

Ruddon R. W. (2007). Cancer biology. *Michigan Medical School, Ann Arbor, Michigan*(Fourth edition), 545.

Ruddon R. W. (2010). Introduction to the molecular biology of cancer: translation to the clinic. *Prog Mol Biol Transl Sci, 95*, 1-8. doi:10.1016/b978-0-12-385071-3.00001-0

Rysman E., Brusselmans K., Scheys K., Timmermans L., Derua R., Munck S., & Swinnen J. V. (2010). De novo lipogenesis protects cancer cells from free radicals and chemotherapeutics by promoting membrane lipid saturation. *Cancer Res, 70*(20), 8117-8126. doi:10.1158/0008-5472.can-09-3871

Sawada M., Nakashima S., Banno Y., Yamakawa H., Takenaka K., Shinoda J., & Nozawa Y. (2000). Influence of Bax or Bcl-2 overexpression on the ceramide-dependent apoptotic pathway in glioma cells. *Oncogene, 19*(31), 3508-3520. doi:10.1038/sj.onc.1203699

Sekharam M., Trotti A., Cunnick J. M., & Wu J. (1998). Suppression of fibroblast cell cycle progression in G1 phase by N-acetylcysteine. *Toxicol Appl Pharmacol, 149*(2), 210-216. doi:10.1006/taap.1997.8361

Semenza G. L. (2011). Regulation of metabolism by hypoxia-inducible factor 1. *Cold Spring Harb Symp Quant Biol, 76*, 347-353. doi:10.1101/sqb.2011.76.010678

Stone J. R., & Collins T. (2002). The role of hydrogen peroxide in endothelial proliferative responses. *Endothelium, 9*(4), 231-238.

Strable M. S., & Ntambi J. M. (2010). Genetic control of de novo lipogenesis: role in diet-induced obesity. *Crit Rev Biochem Mol Biol, 45*(3), 199-214. doi:10.3109/10409231003667500

Sun J., Aluvila S., Kotaria R., Mayor J. A., Walters D. E., & Kaplan R. S. (2010). Mitochondrial and plasma membrane citrate transporters: discovery of selective inhibitors and application to structure/function analysis. *Mol Cell Pharmacol, 2*(3), 101-110.

Thupari J. N., Pinn M. L., & Kuhajda F. P. (2001). Fatty acid synthase inhibition in human breast cancer cells leads to malonyl-CoA-induced inhibition of fatty acid oxidation and cytotoxicity. *Biochem Biophys Res Commun, 285*(2), 217-223. doi:10.1006/bbrc.2001.5146

Tomimaru Y., Koga H., Yano H., de la Monte S., Wands J. R., & Kim M. (2013). Upregulation of T-cell factor-4 isoform-responsive target genes in hepatocellular carcinoma. *Liver Int, 33*(7), 1100-1112. doi:10.1111/liv.12188

Vander Heiden M. G., Cantley L. C., & Thompson C. B. (2009). Understanding the Warburg effect: the metabolic requirements of cell proliferation. *Science, 324*(5930), 1029-1033. doi:10.1126/science.1160809

Wang C., Xu C., Sun M., Luo D., Liao D. F., & Cao D. (2009). Acetyl-CoA carboxylase-alpha inhibitor TOFA induces human cancer cell apoptosis. *Biochem Biophys Res Commun, 385*(3), 302-306. doi:10.1016/j.bbrc.2009.05.045

Xu Y., Kakhniashvili D. A., Gremse D. A., Wood D. O., Mayor J. A., Walters D. E., & Kaplan R. S. (2000). The yeast mitochondrial citrate transport protein. Probing the roles of cysteines, Arg(181), and Arg(189) in transporter function. *J Biol Chem, 275*(10), 7117-7124.

Yuan T. L., & Cantley L. C. (2008). PI3K pathway alterations in cancer: variations on a theme. *Oncogene, 27*(41), 5497-5510. doi:10.1038/onc.2008.245

Zaidi N., Lupien L., Kuemmerle N. B., Kinlaw W. B., Swinnen J. V., & Smans K. (2013). Lipogenesis and lipolysis: the pathways exploited by the cancer cells to acquire fatty acids. *Prog Lipid Res, 52*(4), 585-589. doi:10.1016/j.plipres.2013.08.005

Zhou W., Han W. F., Landree L. E., Thupari J. N., Pinn M. L., Bililign T., & Kuhajda F. P. (2007). Fatty acid synthase inhibition activates AMP-activated protein kinase in SKOV3 human ovarian cancer cells. *Cancer Res, 67*(7), 2964-2971. doi:10.1158/0008-5472.can-06-3439

Zorov D. B., Juhaszova M., & Sollott S. J. (2014). Mitochondrial reactive oxygen species (ROS) and ROS-induced ROS release. *Physiol Rev, 94*(3), doi:10.1152/physrev.00026.2013

APPENDIX

APPENDIX A PREPARATION OF 1X PBS

Table 1 Preparation of 1X PBS

Reagent	Amount (g)
NaCl	8
KCl	0.2
Na2HPO4	1.44
KH2PO4	0.24

Source: http://www.protocolsonline.com/recipes/phosphate-buffered-saline-pbs

Recipe for 1 liter of 1X Phosphate Buffered Saline (PBS Buffer) solution starts with 800 ml of distilled water. Dissolve the solution as described above, and then adjust pH stock is will be approximately 7.4. If necessary, pH can be adjusted using hydrochloric acid or sodium hydroxide. Dispense the solution into aliquots and sterilize by autoclaving (20 min, 121°C, liquid cycle). Store at room temperature.

APPENDIX B PREPARATION OF DILUTED ALBUMIN (BSA)

Assay is a detergent-compatible formulation based on bicinchoninic acid (BCA) for the colorimetric detection and quantitation of total protein. Use Table 2 as a guide to prepare a set of protein standards. Dilute the contents of one Albumin Standard (BSA) ampule into several clean vials, preferably using the same diluent as the samples. Each 1mL ampule of 2000 µg/mL Albumin Standard is sufficient to prepare a set of diluted standards for either working range suggested in Table 2. There will be sufficient volume for three replications of each diluted standard.

Table 2 Preparation of Diluted Albumin (BSA) Standards

Vial	Volume of dH2O (µL)	Volume of BSA (µL)	Final BSA Concentration (µg/mL)
A	0	80	2000
B	40	40	1000
C	60	20	500
D	79	1	25

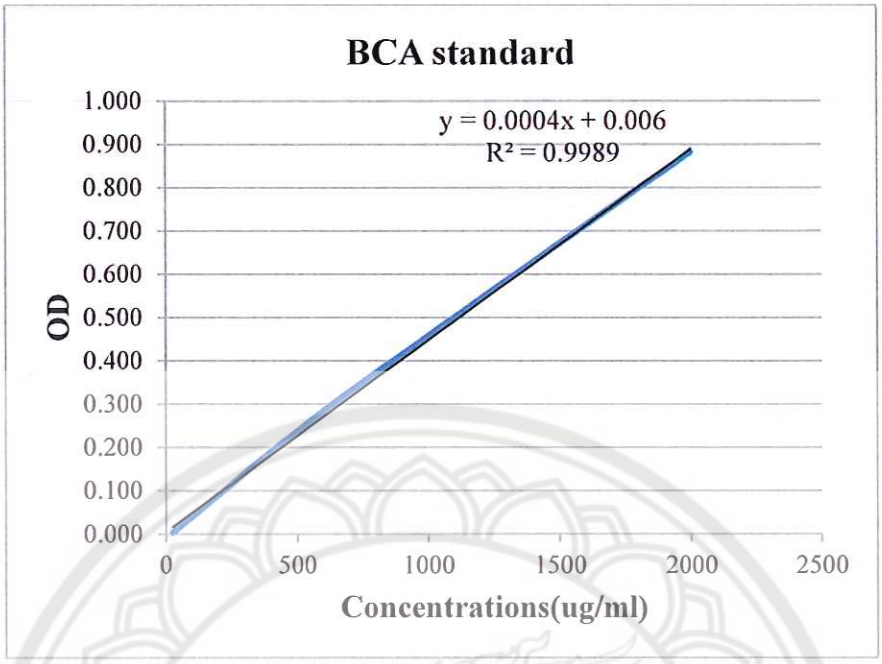

Figure 22 Standard curve involving four points

Source: https://tools.thermofisher.com/content/sfs/manuals/MAN0011430_Pierce_BCA_Protein_Asy_UG

APPENDIX C M-PER® PROTEIN EXTRACTION REAGENT

1. Optional Wash: If the culture medium contained phenol red or other reagents that could interfere with subsequent protein analysis, wash the cells once by resuspending the cell pellet in wash buffer (e.g., PBS). Pellet cells by centrifugation at 2500 × g for 10 minutes.

2. Add M-PER Reagent to the cell pellet. Use at least 1mL of M-PER Reagent for each 100mg (~100µL) of wet cell pellet. If a large amount of cells is used, first add 1/10 the final recommended volume of M-PER Reagent to the cell pellet. Pipette the mixture up and down to resuspend pellet. Add the rest of the M-PER Reagent to the cell suspension.

3. Shake mixture gently for 10 minutes. Remove cell debris by centrifugation at ~14,000 × g for 15 minutes.

4. Transfer the supernatant to a new tube for analysis.

Source: https://tools.thermofisher.com/content/sfs/manuals/MAN0011378_MPER_Mammal_Protein_Extract_Reag_UG

APPENDIX D CITRATE ASSAY KIT

Sample preparation

1. Harvest number of cells for each assay (recommendation 2 x 10^6 cells).
2. Wash cells with cold PBS.
3. Resuspend cells in 100 µL of Assay Buffer.
4. Homogenize cells quickly by pipetting up and down a few times.
5. Centrifuge sample for 2 – 5 minutes at 4°C at top speed using a cold microcentrifuge to remove any insoluble material.
6. Collect supernatant and transfer to a clean tube.
7. Keep on ice.
8. Perform deproteinization step as described in section 5.

Citrate Reaction Mix

Prepare 10X citrate probe dilute to 1X in 100% DMSO

Component	Reaction Mix (µL)
Assay Buffer	44
Enzyme Mix	2
Developer	2
Citrate Probe*	2

*NOTE: For fluorometric readings, using Citrate Probe diluted 10X decreases the fluorescent background readings, therefore increasing detection sensitivity. Mix enough reagents for the number of assays (samples, standards and background control) to be performed. Prepare a master mix of the Reaction Mix to ensure consistency. Recommend the following calculation: X µL component x (Number samples) Add 50 µL of Background Reaction Mix into background sample control well. Incubate at room temperature for 30 min protected from light and measure output on a microplate reader: Fluorometric assay: measure Ex/Em = 535/587 nm.

Source: http://www.abcam.com/citrate-assay-kit-ab83396.html

APPENDIX E FATTY ACID QUANTIFICATION ASSAY KIT

Sample preparation

1. Harvest number of cells for each assay (recommendation 2 x 10^6 cells).
2. Wash cells with cold PBS.
3. Homogenize cells in 200 µL chloroform/Triton X-100 in pure chloroform by pipetting up and down or using a micro-homogenizer. Incubate on ice 10 – 30 minutes.
4. Spin the extract for 5 – 10 minutes at top speed in a microcentrifuge.
5. Collect organic phase (lower phase), air dry at 50°C in a fume hood to remove chloroform.
6. Vacuum dry for 30 minutes to remove trace chloroform.
7. Dissolve the dried lipids in 200 µL of Fatty Acid Assay Buffer by vortexing extensively for 5 minutes.

Reaction Mix (FLUOROMETRIC ASSAY)

Prepare 50 µL Reaction Mix for each reaction: Mix enough reagents for the number of assays (samples and controls) to be performed. Prepare a master mix of the Reaction Mix to ensure consistency. We recommend the following calculation: X µL component x (Number reactions +1).

Component	Reaction Mix (µL)
Assay Buffer	45.6
Fatty Acid Probe*	0.4
Enzyme Mix	2
Enhancer	2

*NOTE: For fluorometric readings, using 0.4 µL/well of the Fatty Acid probe decreases the background readings, therefore increasing detection sensitivity. Add 50 µL of Reaction Mix to each well. Incubate at 37°C for 30 minutes protected from light. Measure output on a microplate reader at Ex/Em 535/587 nm.

Source: http://www.abcam.com/free-fatty-acid-quantification-kit-ab65341.html

APPENDIX F TRIGLYCERIDE QUANTIFICATION ASSAY KIT

Sample preparation

1. Harvest number of cells for each assay (recommendation 2 x 10^6 cells).
2. Wash cells with cold PBS.
3. Resuspend and homogenize samples in 1 mL of 5% NP-40/ dH_2O solution.
4. Slowly heat the samples to 80 – 100°C in a water bath for 2 –5 minutes or until the NP-40 becomes cloudy, then cool down to room temperature.
5. Repeat previous step to solubilize all triglyceride.
6. Centrifuge for 2 minutes at top speed using a microcentrifuge to remove any insoluble material.
7. Dilute samples 10-fold with dH_2O before proceeding with the assay.

Triglyceride Reaction Mix

Prepare 50 µL of Reaction Mix for each reaction. Mix enough reagents for the number of assays (samples, standards and background control) to be performed. Prepare a Master Mix of the Reaction Mix to ensure consistency. We recommend the following calculation: X µL component x (Number reactions + 1)

Component	Reaction Mix (µL)
Triglyceride Assay buffer	47.6
Triglyceride Probe*	0.4
Triglyceride Enzyme Mix	2

*NOTE: for fluorometric readings, using 0.4 µL/well of the triglyceride probe decreases the background readings, therefore increasing detection sensitivity.

Add 50 µL of Reaction Mix into each well. Mix and incubate at room temperature for 60 minutes protected from light. Measure output on a microplate reader at Ex/Em = 535/587 nm for a fluorometric assay. The reaction is stable for at least two hours.

Source: http://www.abcam.com/triglyceride-quantification-kit-ab65336.html